Supplementary Material for: Assessing the domain-based local pair orbital (DLPNO) approximation for non-covalent interactions in sizable supramolecular complexes

Montgomery Gray and John M. Herbert*

Department of Chemistry & Biochemistry
The Ohio State University, Columbus, Ohio 43210 USA

July 6, 2024

Contents

S1 Data for S66 **S4**
S1.1 DLPNO errors: RI-MP2 with Dunning basis sets . . . S4
S1.1.1 Absolute errors . . . S4
S1.1.2 Extrapolated errors . . . S6
S1.1.3 Error histograms . . . S8
S1.2 DLPNO errors: RI-MP2 with Karlsruhe basis sets . . . S10
S1.2.1 Absolute errors . . . S10
S1.2.2 Extrapolated errors . . . S12
S1.2.3 Error histograms . . . S14
S1.3 DLPNO errors in RI-MP2 correlation energies . . . S16
S1.4 MP2/CBS extrapolations . . . S22
S1.5 Convergence with PNO threshold . . . S24
S1.5.1 RI-MP2 with Dunning basis sets . . . S24
S1.5.2 RI-MP2 with Karlsruhe basis sets . . . S26
S1.5.3 CCSD(T) data . . . S28

S2 Data for Larger Complexes **S30**
S2.1 RI-MP2 with Karlsruhe basis sets . . . S30
S2.2 RI-MP2 with Dunning basis sets . . . S35
S2.3 CCSD(T) . . . S37

List of Figures

S1 Absolute DLPNO errors with respect to canonical RI-MP2 interaction energies for the S66 dataset using cc-pVXZ and PNO thresholds as indicated. . . . S4

*herbert@chemistry.ohio-state.edu

S2 Absolute DLPNO errors with respect to canonical RI-MP2 interaction energies for the S66 dataset using aug-cc-pVXZ and PNO thresholds as indicated. S5
S3 Absolute DLPNO errors for S66 using cc-pVXZ basis sets, based on extrapolation using data with the indicated thresholds. S6
S4 Absolute DLPNO errors for S66 using aug-cc-pVXZ basis sets, based on extrapolation using data with the indicated thresholds. S7
S5 Counts of the absolute DLPNO errors (with respect to canonical RI-MP2 interaction energies) for S66, using cc-pVXZ basis sets and PNO thresholds as indicated. S8
S6 Counts of the absolute DLPNO errors (with respect to canonical RI-MP2 interaction energies) for S66, using aug-cc-pVXZ basis sets and PNO thresholds as indicated. S9
S7 Absolute DLPNO errors with respect to canonical RI-MP2 interaction energies, for S66 using def2-SVP and def2-TZVP, with PNO thresholds as indicated. S10
S8 Absolute DLPNO errors with respect to canonical RI-MP2 interaction energies, for S66 using def2-SVPD and def2-TZVPD, with PNO thresholds as indicated. S11
S9 Absolute DLPNO errors for S66, using def2-SVP and def2-TZVP, based on extrapolation using data with the indicated thresholds. S12
S10 Absolute DLPNO errors for S66, using def2-SVPD and def2-TZVPD, based on extrapolation using data with the indicated thresholds. S13
S11 Counts of the absolute DLPNO errors (with respect to canonical RI-MP2 interaction energies) for S66, using def2-SVP and def2-TZVP and PNO thresholds as indicated. S14
S12 Counts of the absolute DLPNO errors (with respect to canonical RI-MP2 interaction energies) for S66, using def2-SVPD and def2-TZVPD and PNO thresholds as indicated. S15
S13 DLPNO errors in correlation energies for the S66 dimers, computed at the RI-MP2/cc-pVXZ level with PNO thresholds as indicated. S16
S14 DLPNO errors in correlation energies monomer #1 of the S66 complexes, computed at the RI-MP2/cc-pVXZ level with PNO thresholds as indicated. S17
S15 DLPNO errors in correlation energies monomer #2 of the S66 complexes, computed at the RI-MP2/cc-pVXZ level with PNO thresholds as indicated. S18
S16 DLPNO errors in correlation energies for the S66 dimers, computed at the RI-MP2/aug-cc-pVXZ level with PNO thresholds as indicated. S19
S17 DLPNO errors in correlation energies monomer #1 of the S66 complexes, computed at the RI-MP2/aug-cc-pVXZ level with PNO thresholds as indicated. S20
S18 DLPNO errors in correlation energies monomer #2 of the S66 complexes, computed at the RI-MP2/aug-cc-pVXZ level with PNO thresholds as indicated. S21
S19 (a) Absolute and (b) percent differences between CBS-extrapolated RI-MP2 interaction energies for the S66 dimers, comparing cc-pV[T/Q]Z extrapolation to aug-cc-pV[T/Q] extrapolation. Standard subsets of S66 are color-coded as in Figs. 3 and 5. . . . . S22
S20 (a) Absolute and (b) percent differences between RI-MP2/cc-pV[D/T]Z and RI-MP2/aug-cc-pV[D/T]Z interaction energies for the S66 dimers, illustrating the impact of diffuse functions on the CBS extrapolation. Standard subsets of S66 are color-coded as in Figs. 3 and 5. . . . S23
S21 Absolute DLPNO errors in RI-MP2/cc-pVXZ interaction energies for the S66 complexes. . . S24
S22 Percentage DLPNO errors in RI-MP2/cc-pVXZ interaction energies for the S66 complexes. . S25
S23 Absolute DLPNO errors in RI-MP2 interaction energies for the S66 complexes, using Karlsruhe basis sets. S26
S24 Percentage DLPNO errors in RI-MP2 interaction energies for the S66 complexes, using Karlsruhe basis sets. S27
S25 Percentage DLPNO errors in (a) CCSD(T_0)/cc-pVDZ versus (b) RI-MP2/cc-pVDZ interaction energies for the S66 complexes, using thresholds for CCSD(T). S28
S26 DLPNO error with respect to the canonical CCSD(T) interaction energies for S66, where the DLPNO-CCSD(T_1) and DLPNO-CCSD(T_0) approximations are used. S29

S27 (a) Absolute and (b) percent DLPNO errors in RI-MP2/Karlsruhe interaction energies for the L7 + BBR data set, as a function of the PNO threshold. S30
S28 (a) Absolute and (b) percent DLPNO errors in RI-MP2/def2-SVP interaction energies for the S12L complexes, as a function of the PNO threshold. S31
S29 (a) Absolute and (b) percent DLPNO errors for L7 + BBR interaction energies, computed at the RI-MP2/def2-SVP level. S32
S30 (a) Absolute and (b) percent DLPNO errors for the L7 + BBR data set, computed at the RI-MP2/def2-SVPD level. S33
S31 (a) Absolute and (b) percent DLPNO errors for the S12L complexes, computed at the RI-MP2/def2-SVPD level. S34
S32 DLPNO errors, as percentages of ΔE for the L7 + BBR complexes, computed at the RI-MP2/cc-pVXZ level. S35
S33 (a) Absolute and (b) percentage differences between extrapolated DLPNO interaction energies and canonical RI-MP2/jun-cc-pVDZ results, for the L7 complexes. S35
S34 (a) Absolute and (b) percentage differences between extrapolated DLPNO interaction energies and canonical RI-MP2/jun-cc-pVDZ results, for the S12L complexes. S36

List of Tables

S1 DLPNO-CCSD(T)/cc-pVDZ interaction energies (in kcal/mol) for the L7 complexes. S37

S1 Data for S66

S1.1 DLPNO errors: RI-MP2 with Dunning basis sets

S1.1.1 Absolute errors

In this section, the notation l-/n-/t-MP2 means loose/normal/tight PNO thresholds as defined for MP2 calculations (see Section II C). Similarly, l-/n-/t-CCSD(T) means loose/normal/tight PNO thresholds as defined for CCSD(T) calculations. We test both sets of thresholds even though the calculations reported here are performed at the RI-MP2 level.

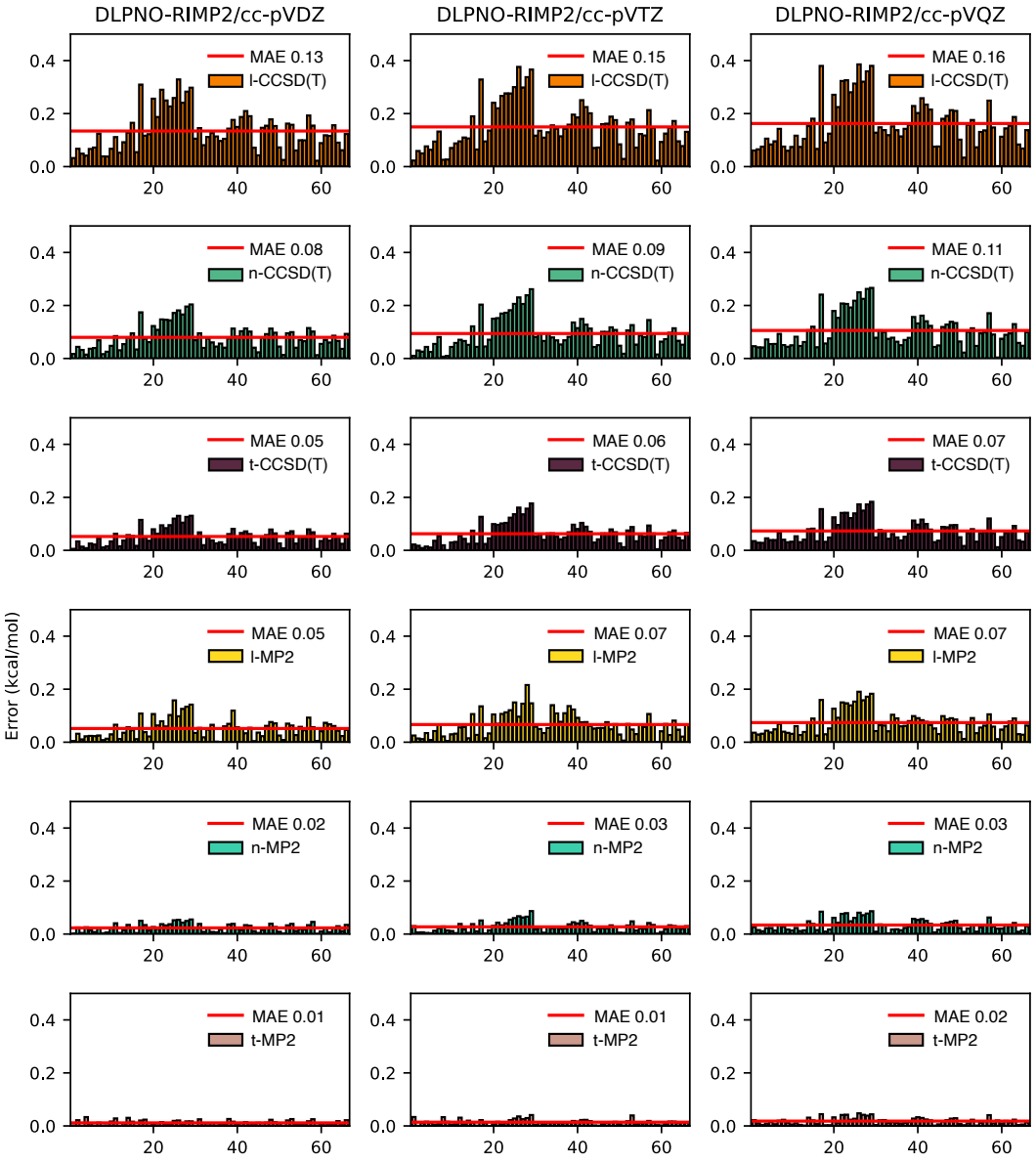

Fig. S1: Absolute DLPNO errors with respect to canonical RI-MP2 interaction energies for the S66 dataset using cc-pVXZ and PNO thresholds as indicated.

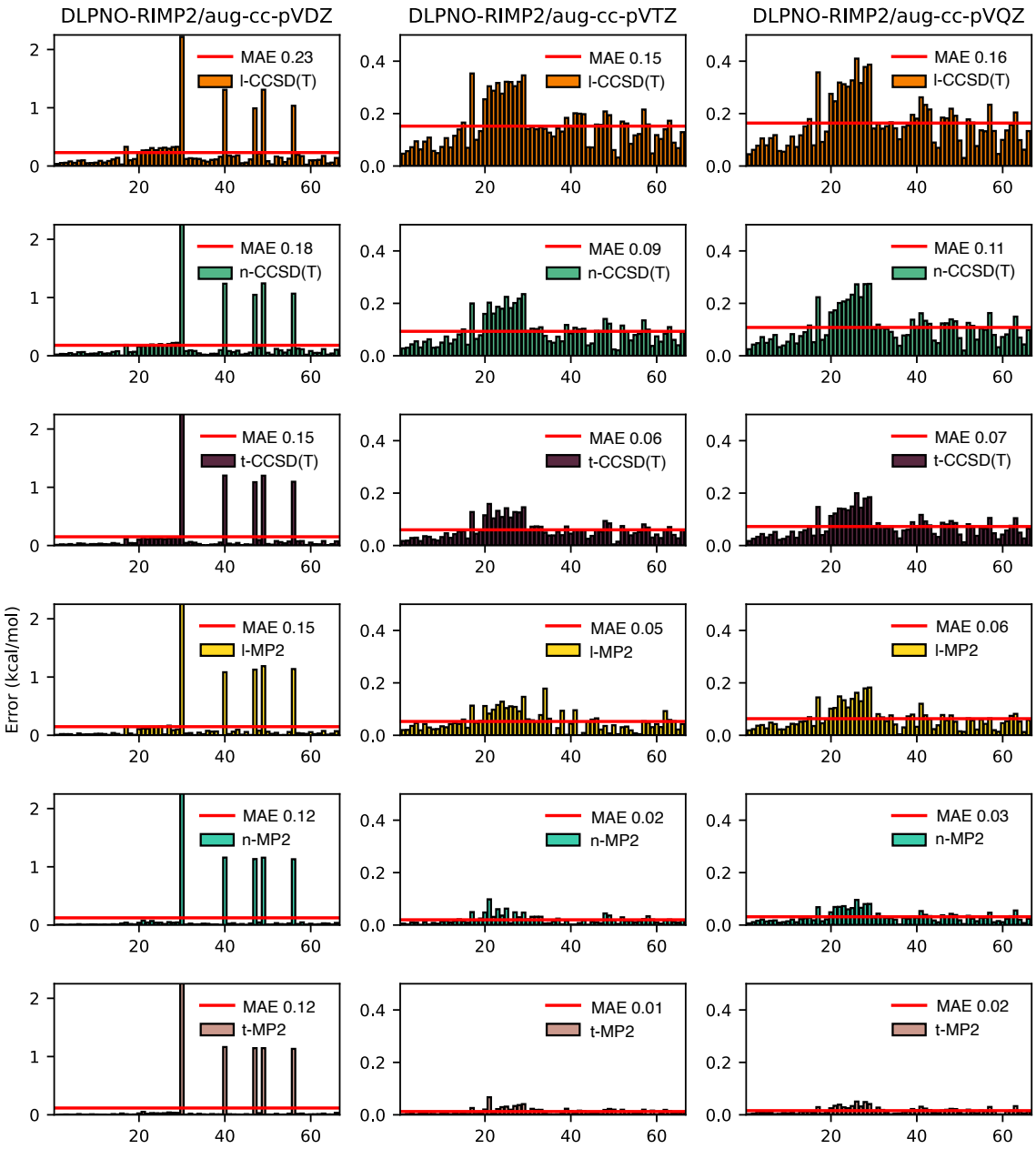

Fig. S2: Absolute DLPNO errors with respect to canonical RI-MP2 interaction energies for the S66 dataset using aug-cc-pVXZ and PNO thresholds as indicated.

S1.1.2 Extrapolated errors

In the graphs below, we indicate loose (l), normal (n), or tight (t) thresholds at either the CCSD(T) or the MP2 level (see Section II C).

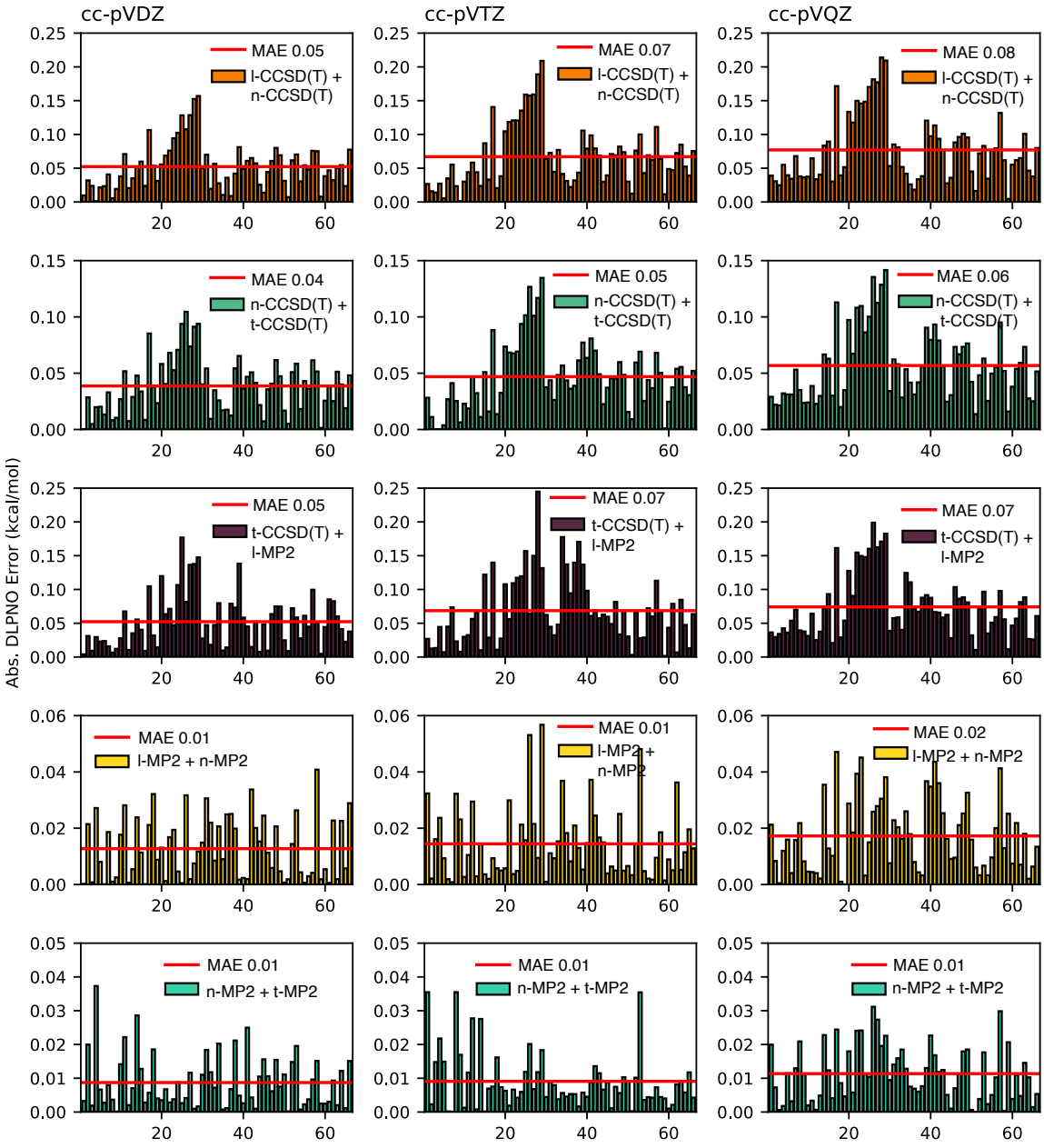

Fig. S3: Absolute DLPNO errors for S66 using cc-pVXZ basis sets, based on extrapolation using data with the indicated thresholds.

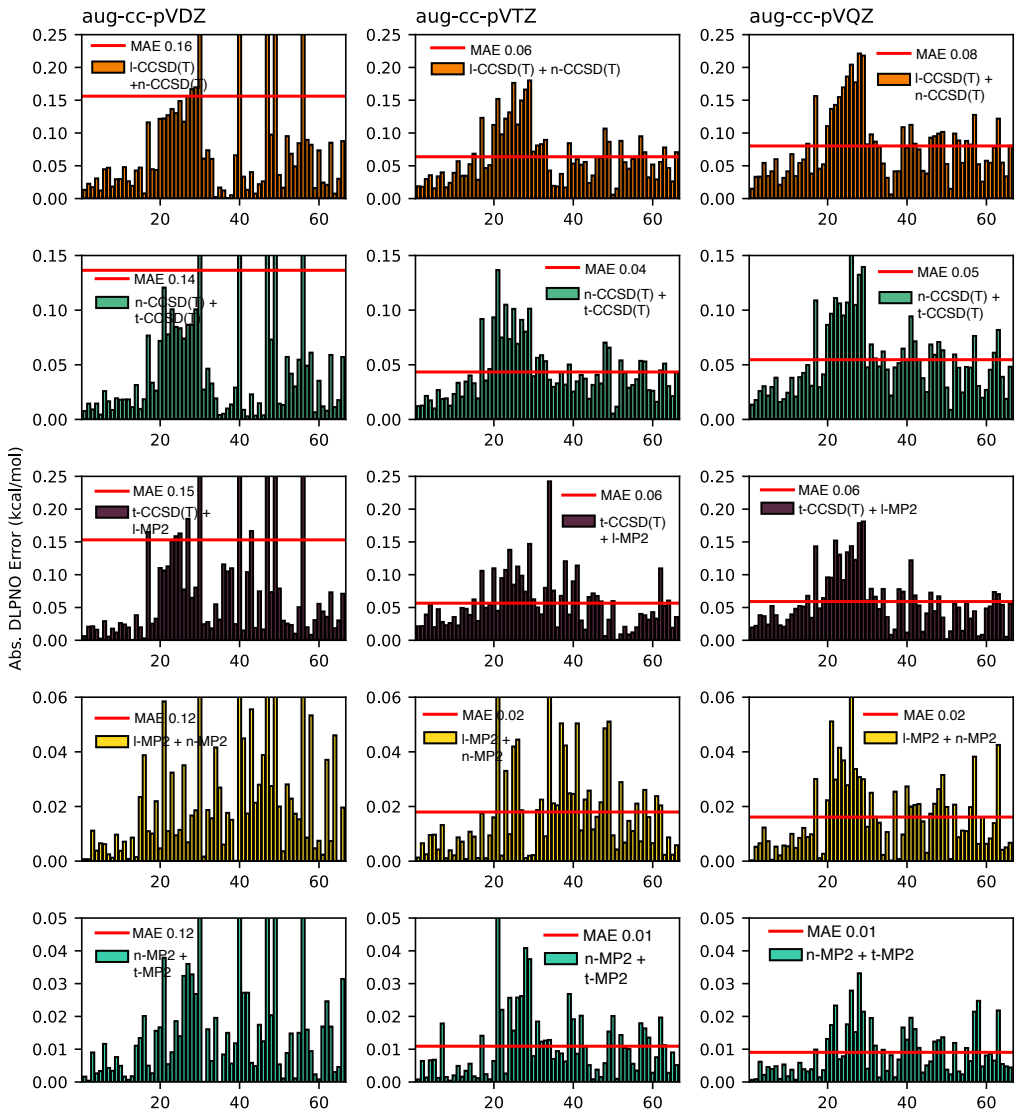

Fig. S4: Absolute DLPNO errors for S66 using aug-cc-pVXZ basis sets, based on extrapolation using data with the indicated thresholds.

S1.1.3 Error histograms

PNO thresholds are indicated as l-/n-/t-MP2 when set at suggested loose/normal/tight values for MP2, or l-/n-/t-CCSD(T) when set at suggested values for CCSD(T), even though all calculations are performed at the RI-MP2 level.

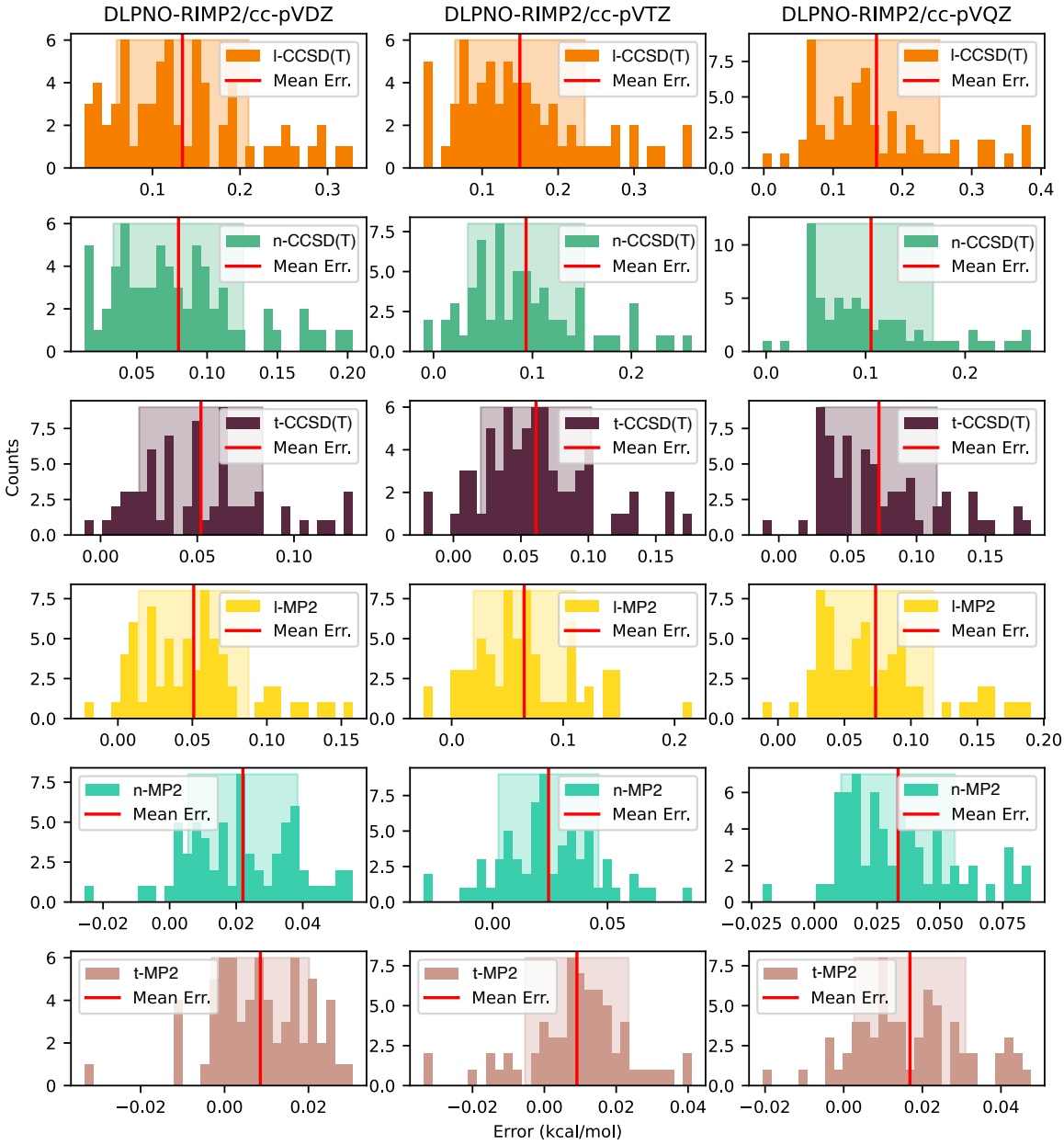

Fig. S5: Counts of the absolute DLPNO errors (with respect to canonical RI-MP2 interaction energies) for S66, using cc-pVXZ basis sets and PNO thresholds as indicated.

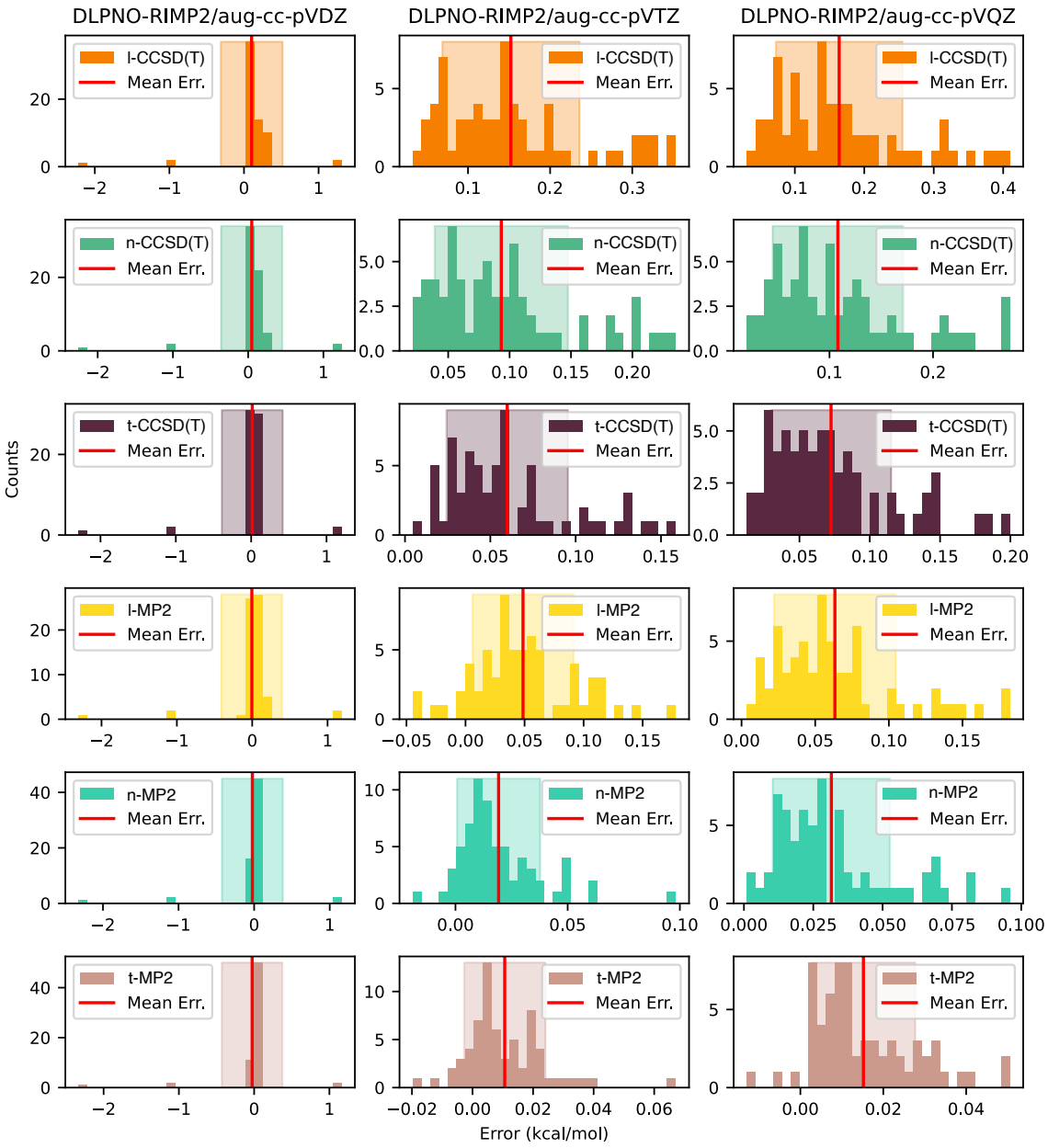

Fig. S6: Counts of the absolute DLPNO errors (with respect to canonical RI-MP2 interaction energies) for S66, using aug-cc-pVXZ basis sets and PNO thresholds as indicated.

S1.2 DLPNO errors: RI-MP2 with Karlsruhe basis sets

S1.2.1 Absolute errors

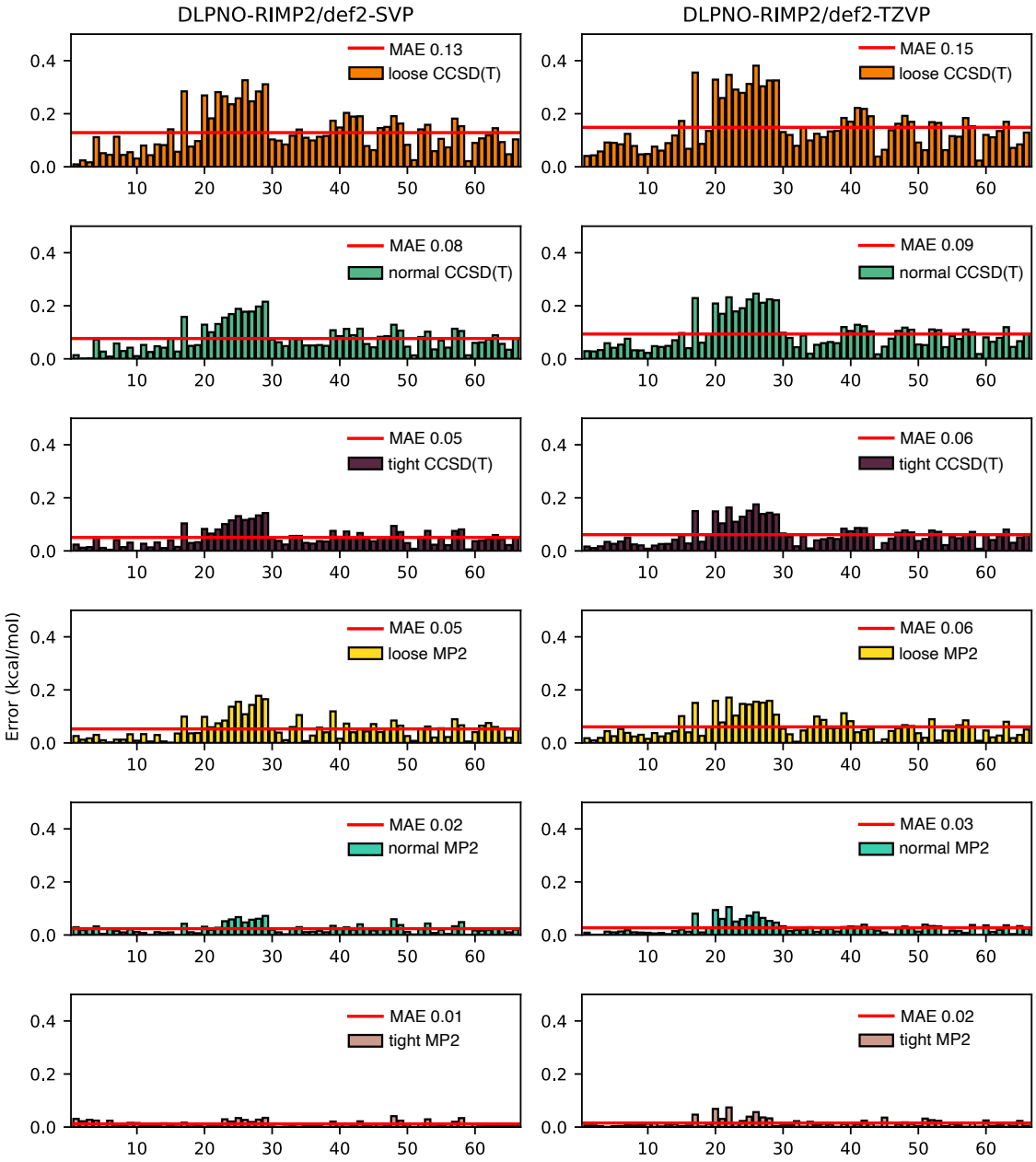

Fig. S7: Absolute DLPNO errors with respect to canonical RI-MP2 interaction energies, for S66 using def2-SVP and def2-TZVP, with PNO thresholds as indicated.

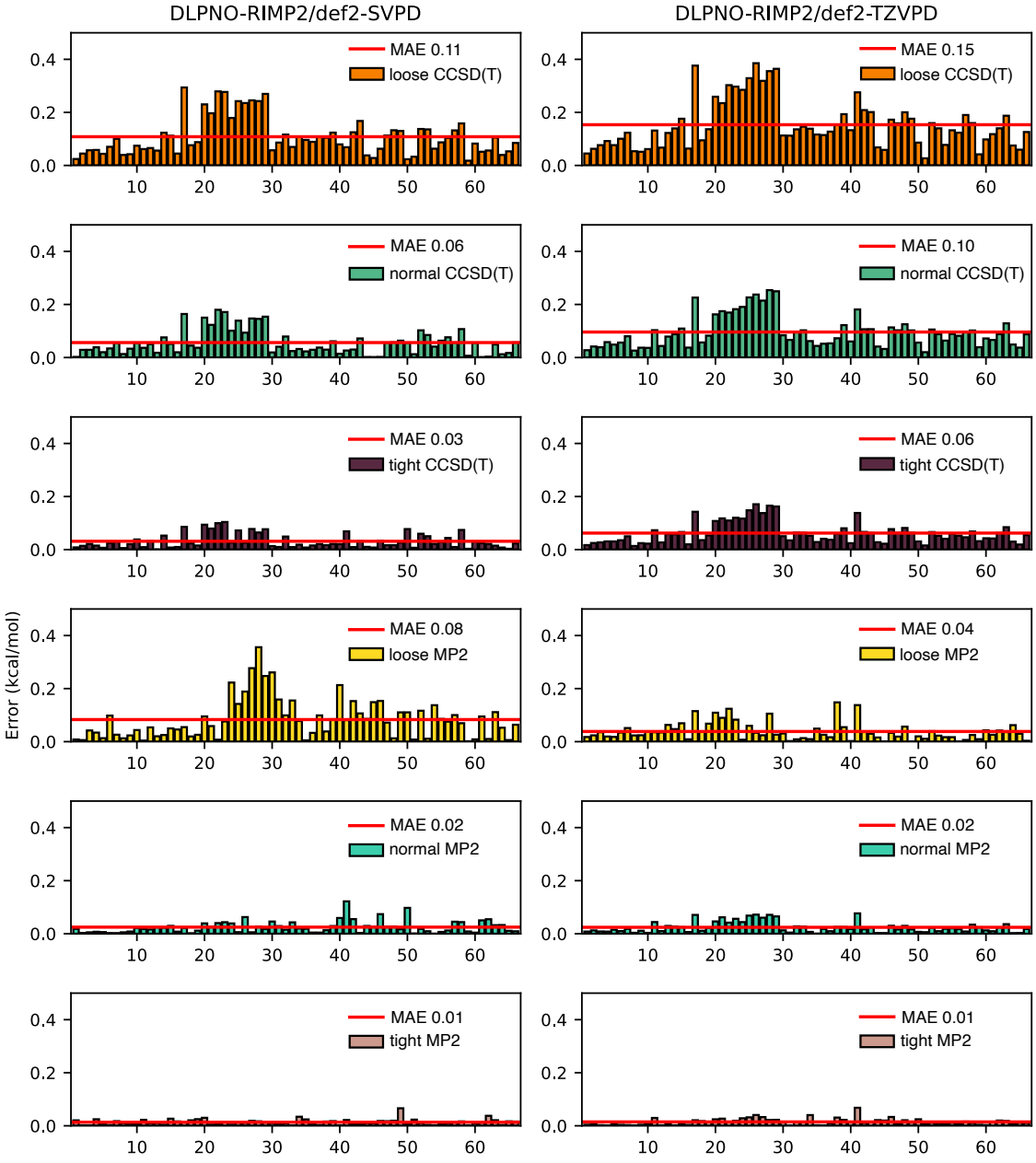

Fig. S8: Absolute DLPNO errors with respect to canonical RI-MP2 interaction energies, for S66 using def2-SVPD and def2-TZVPD, with PNO thresholds as indicated.

S1.2.2 Extrapolated errors

In the graphs below, we indicate loose (l), normal (n), or tight (t) thresholds at either the CCSD(T) or the MP2 level (see Section II C).

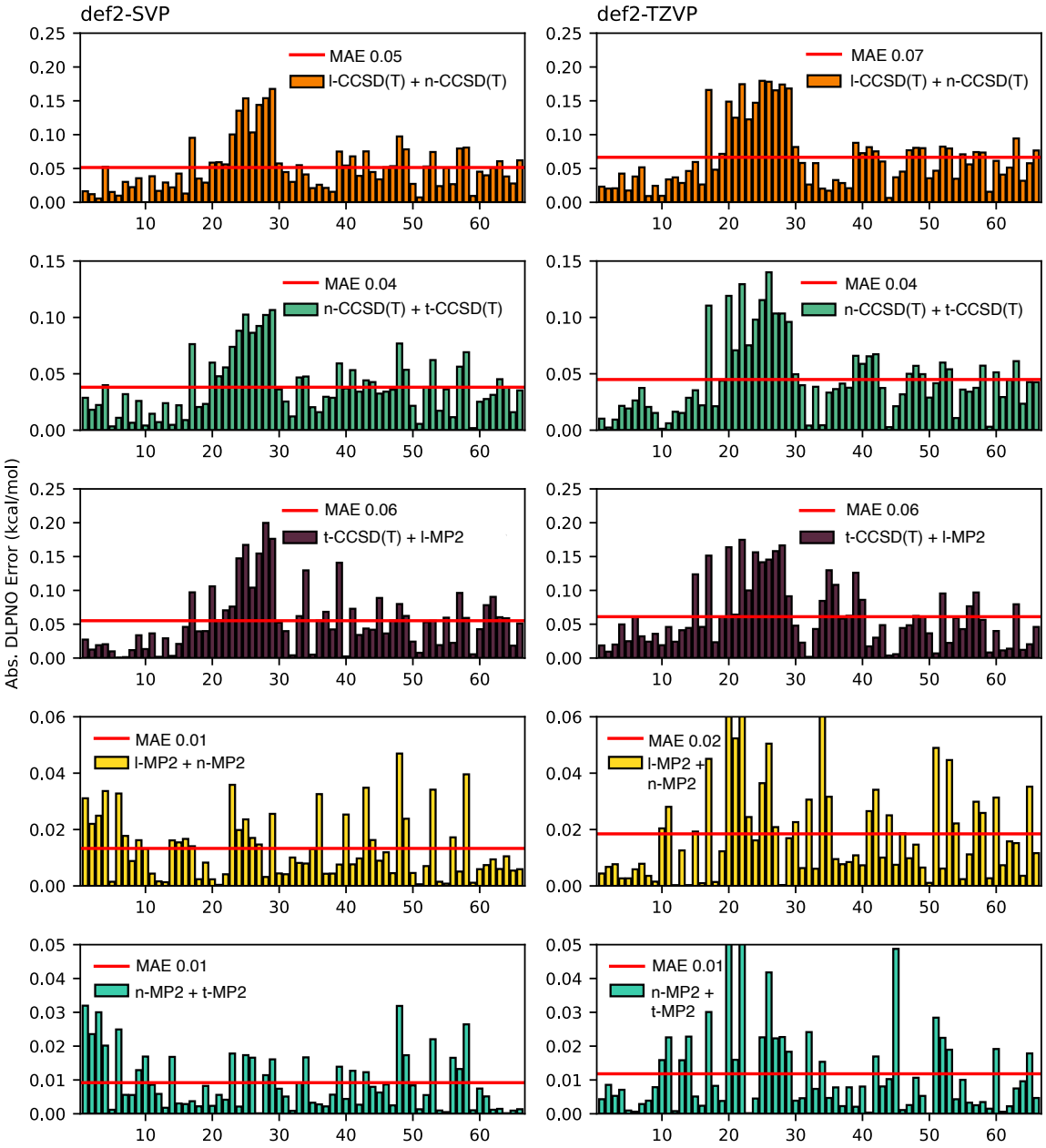

Fig. S9: Absolute DLPNO errors for S66, using def2-SVP and def2-TZVP, based on extrapolation using data with the indicated thresholds.

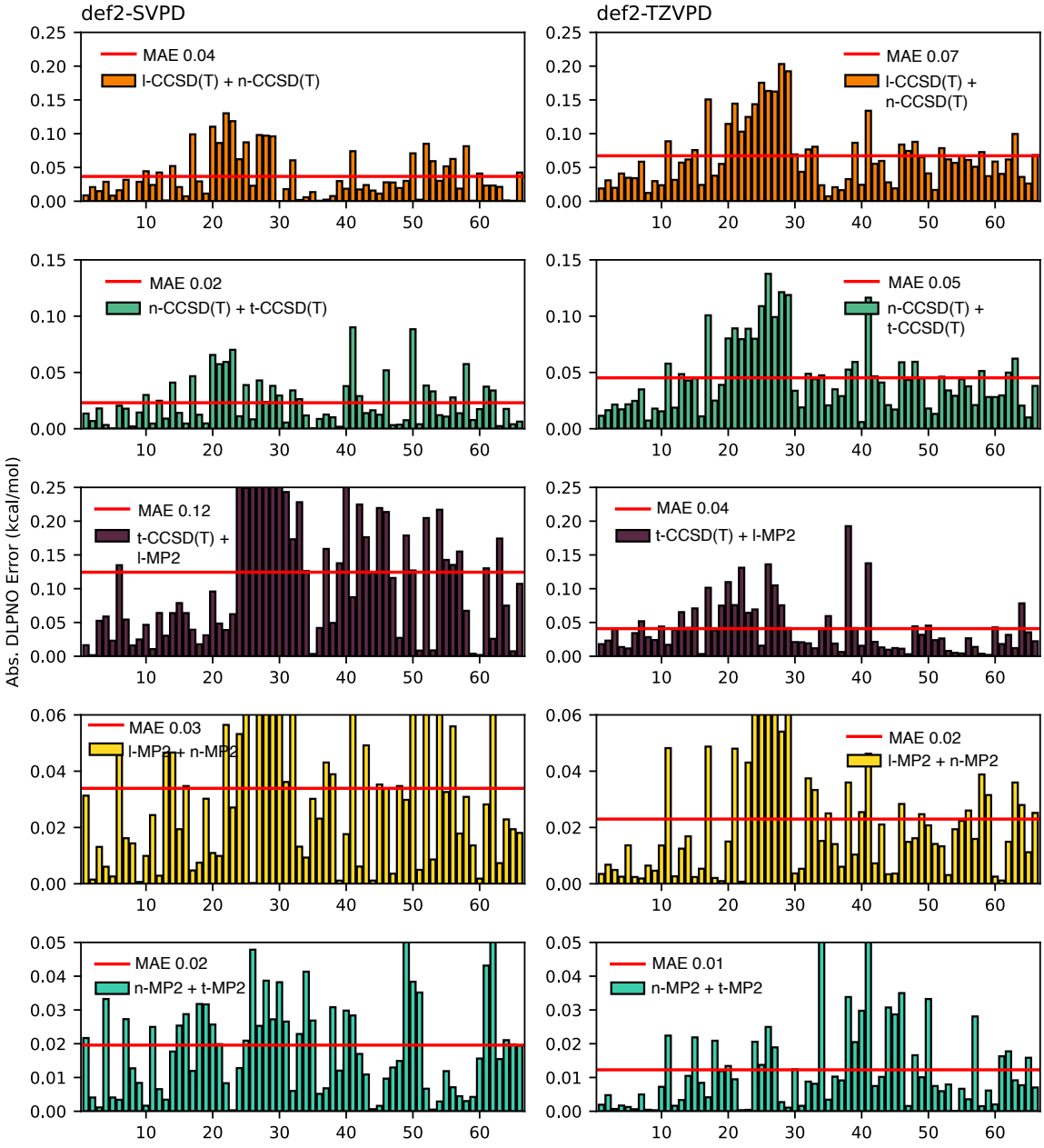

Fig. S10: Absolute DLPNO errors for S66, using def2-SVPD and def2-TZVPD, based on extrapolation using data with the indicated thresholds.

S1.2.3 Error histograms

PNO thresholds are indicated as l-/n-/t-MP2 when set at suggested loose/normal/tight values for MP2, or l-/n-/t-CCSD(T) when set at suggested values for CCSD(T), even though all calculations are performed at the RI-MP2 level.

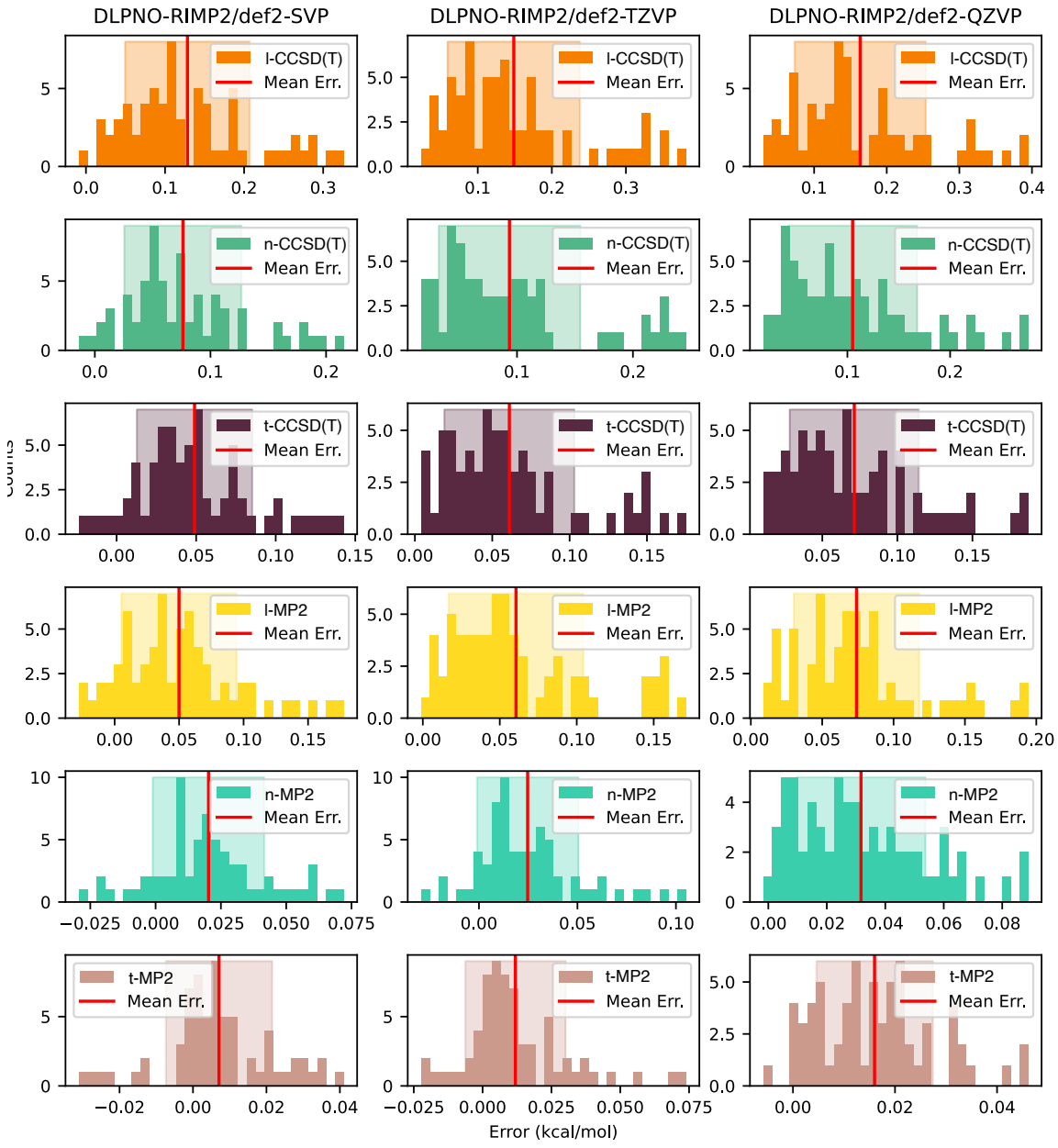

Fig. S11: Counts of the absolute DLPNO errors (with respect to canonical RI-MP2 interaction energies) for S66, using def2-SVP and def2-TZVP and PNO thresholds as indicated.

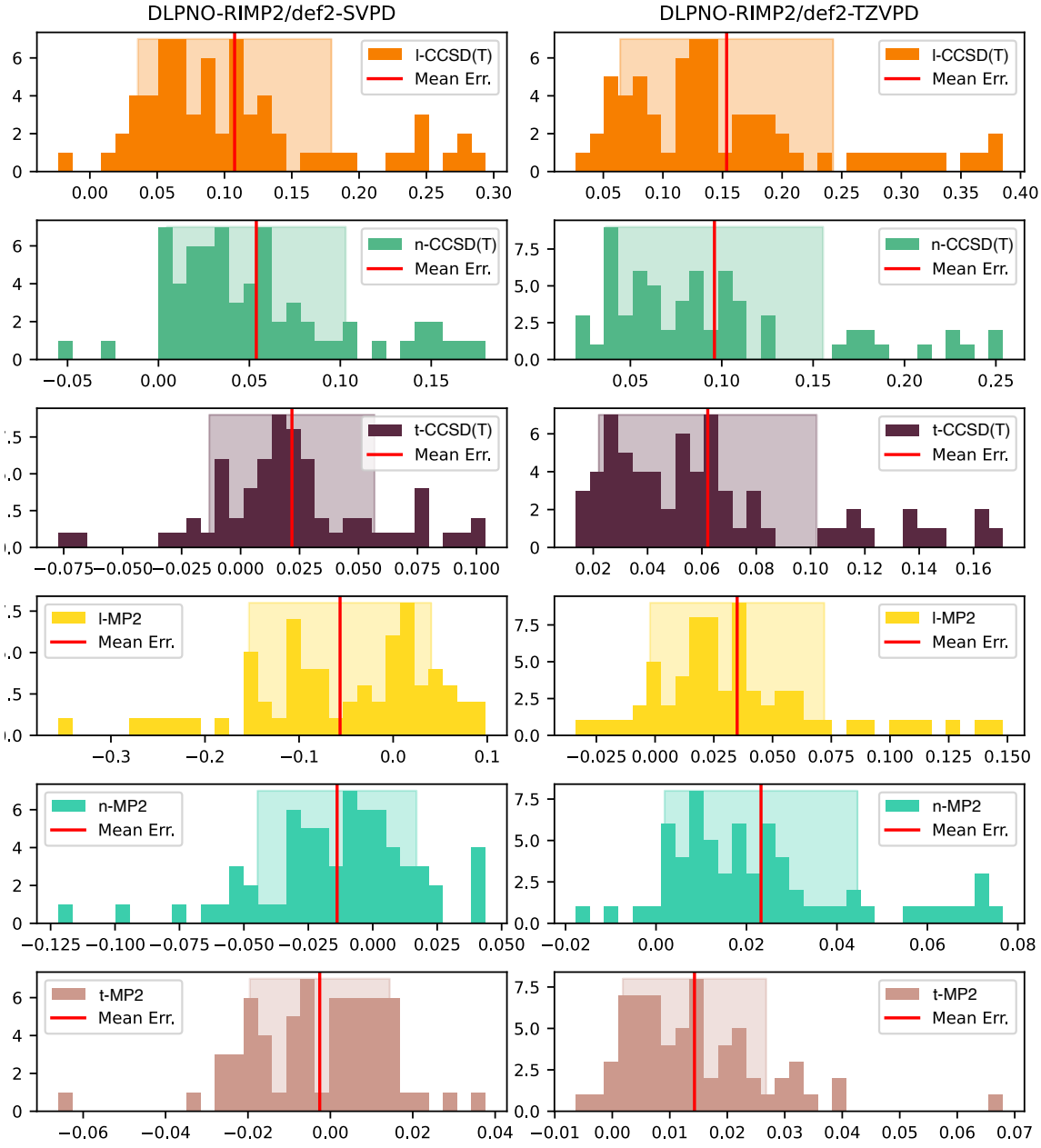

Fig. S12: Counts of the absolute DLPNO errors (with respect to canonical RI-MP2 interaction energies) for S66, using def2-SVPD and def2-TZVPD and PNO thresholds as indicated.

S1.3 DLPNO errors in RI-MP2 correlation energies

These calculations are performed with various PNO thresholds, including those typical of CCSD(T), even though all calculations are RI-MP2.

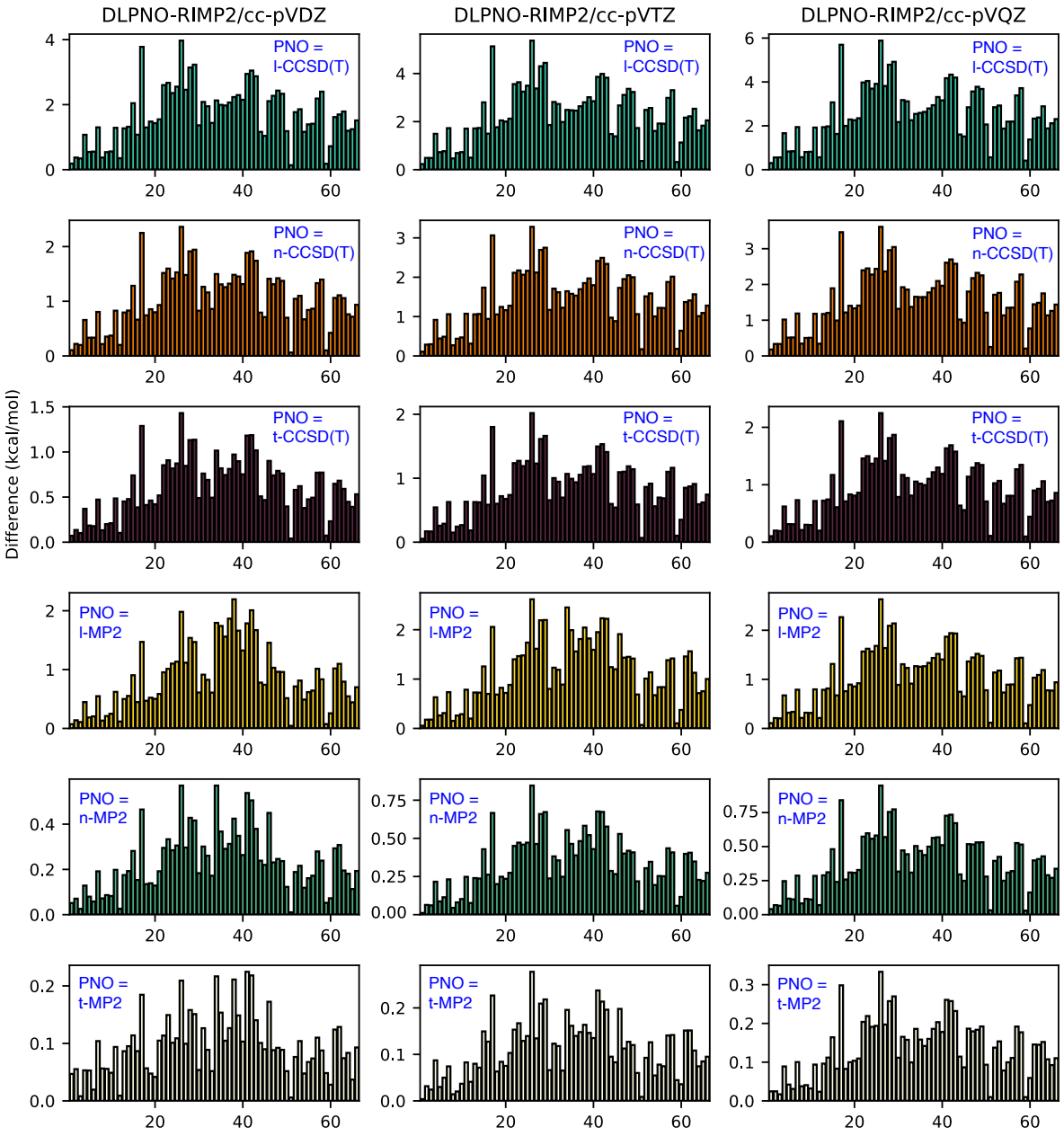

Fig. S13: DLPNO errors in correlation energies for the S66 dimers, computed at the RI-MP2/cc-pVXZ level with PNO thresholds as indicated.

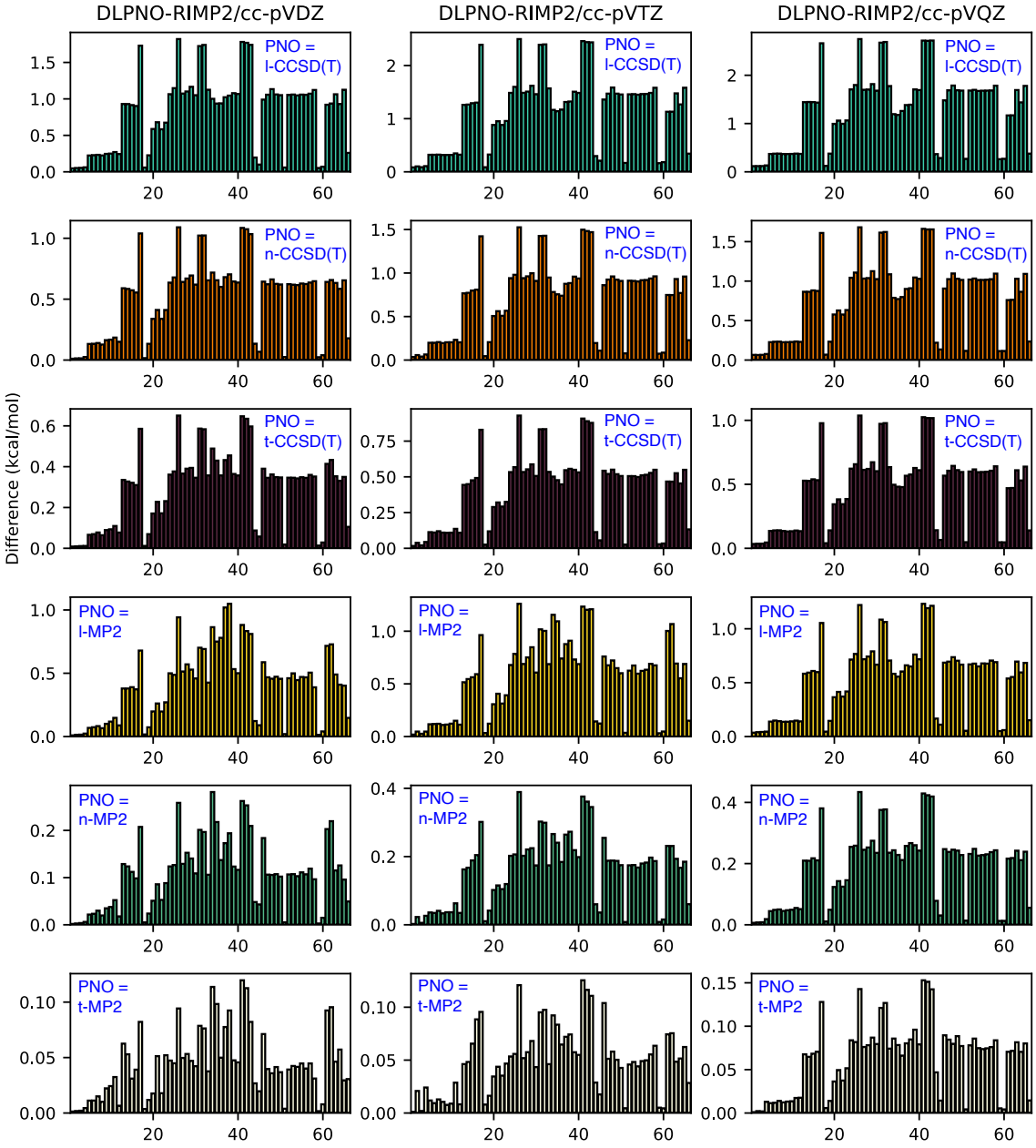

Fig. S14: DLPNO errors in correlation energies monomer #1 of the S66 complexes, computed at the RI-MP2/cc-pVXZ level with PNO thresholds as indicated.

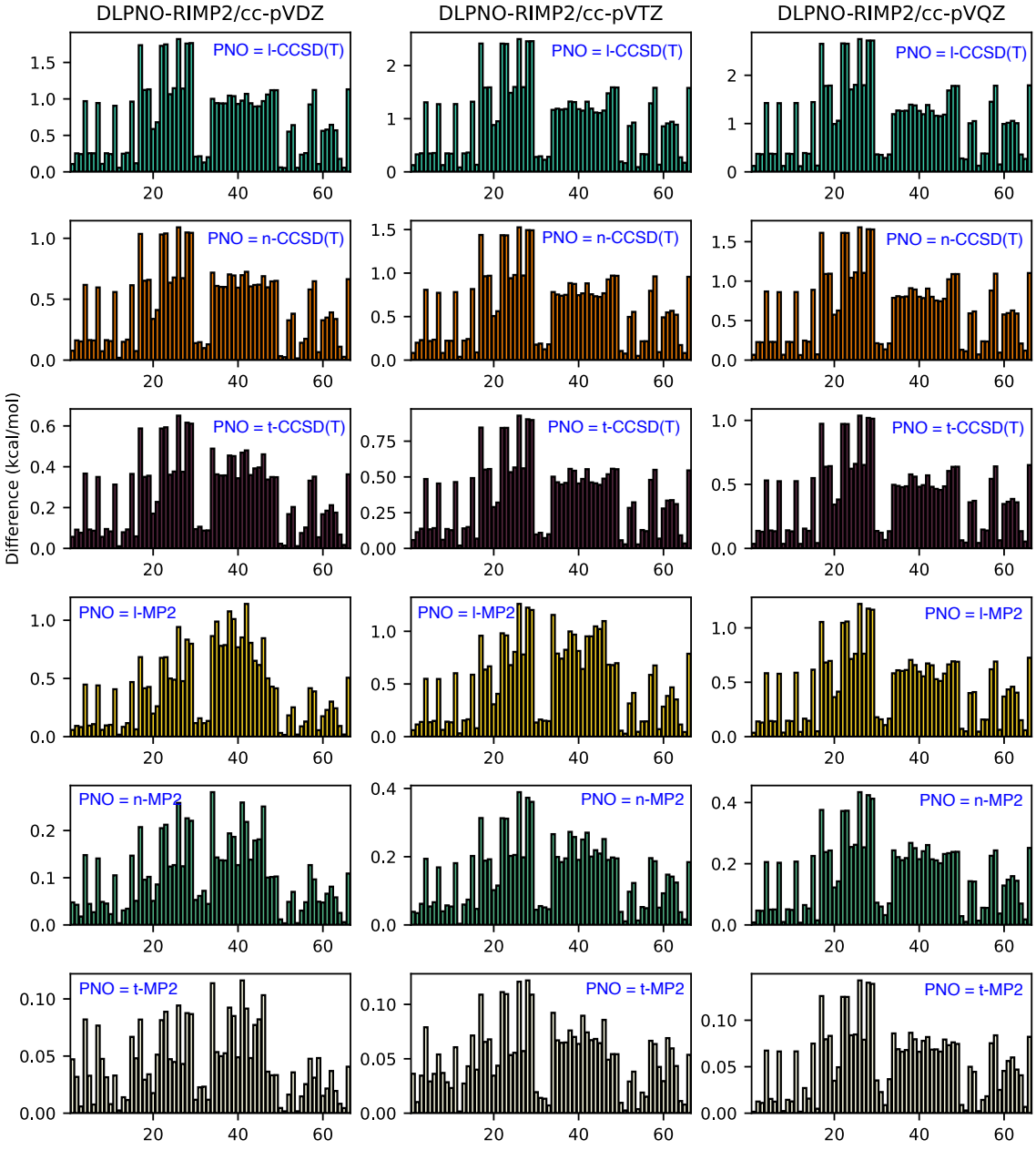

Fig. S15: DLPNO errors in correlation energies monomer #2 of the S66 complexes, computed at the RI-MP2/cc-pVXZ level with PNO thresholds as indicated.

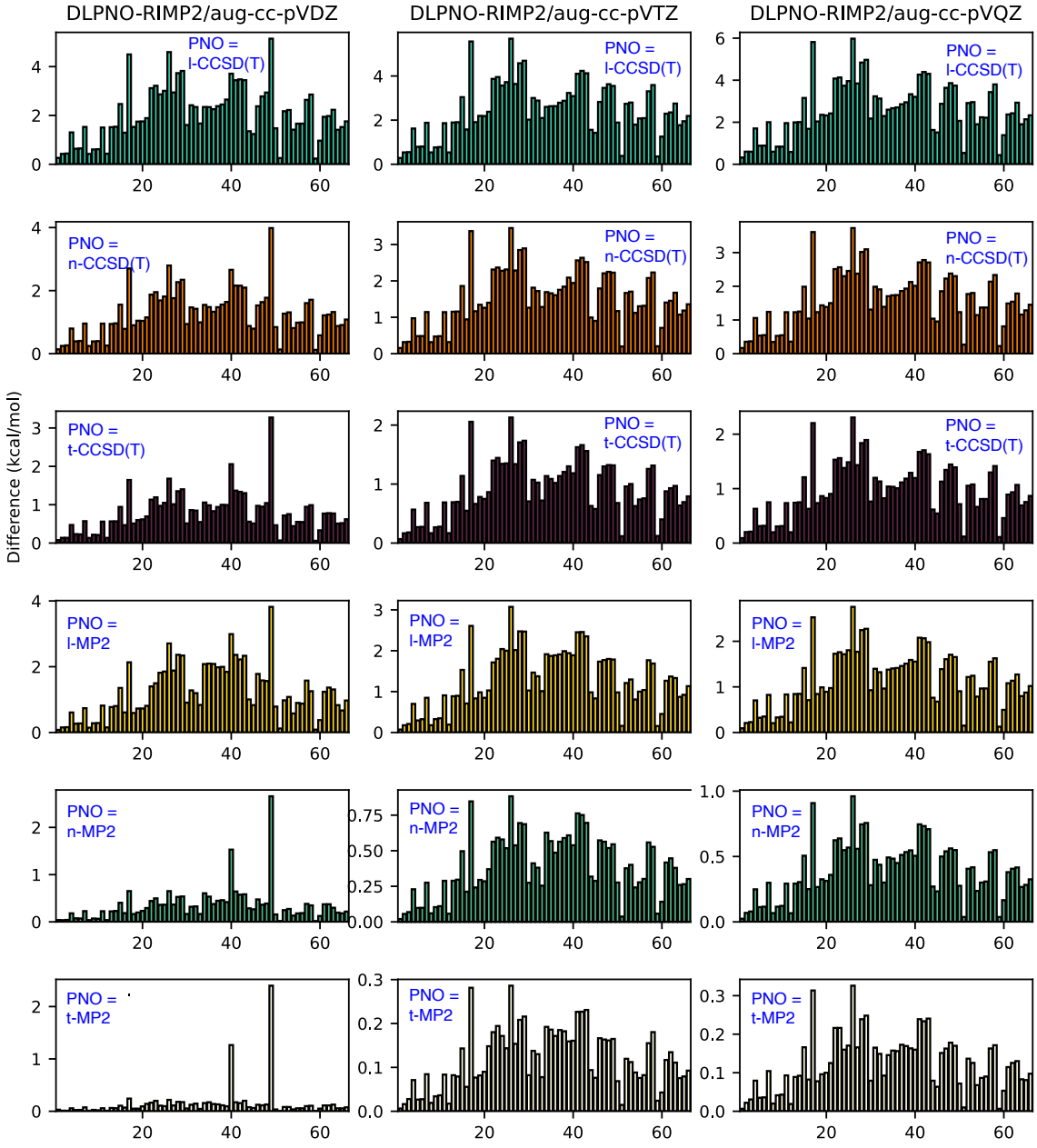

Fig. S16: DLPNO errors in correlation energies for the S66 dimers, computed at the RI-MP2/aug-cc-pVXZ level with PNO thresholds as indicated.

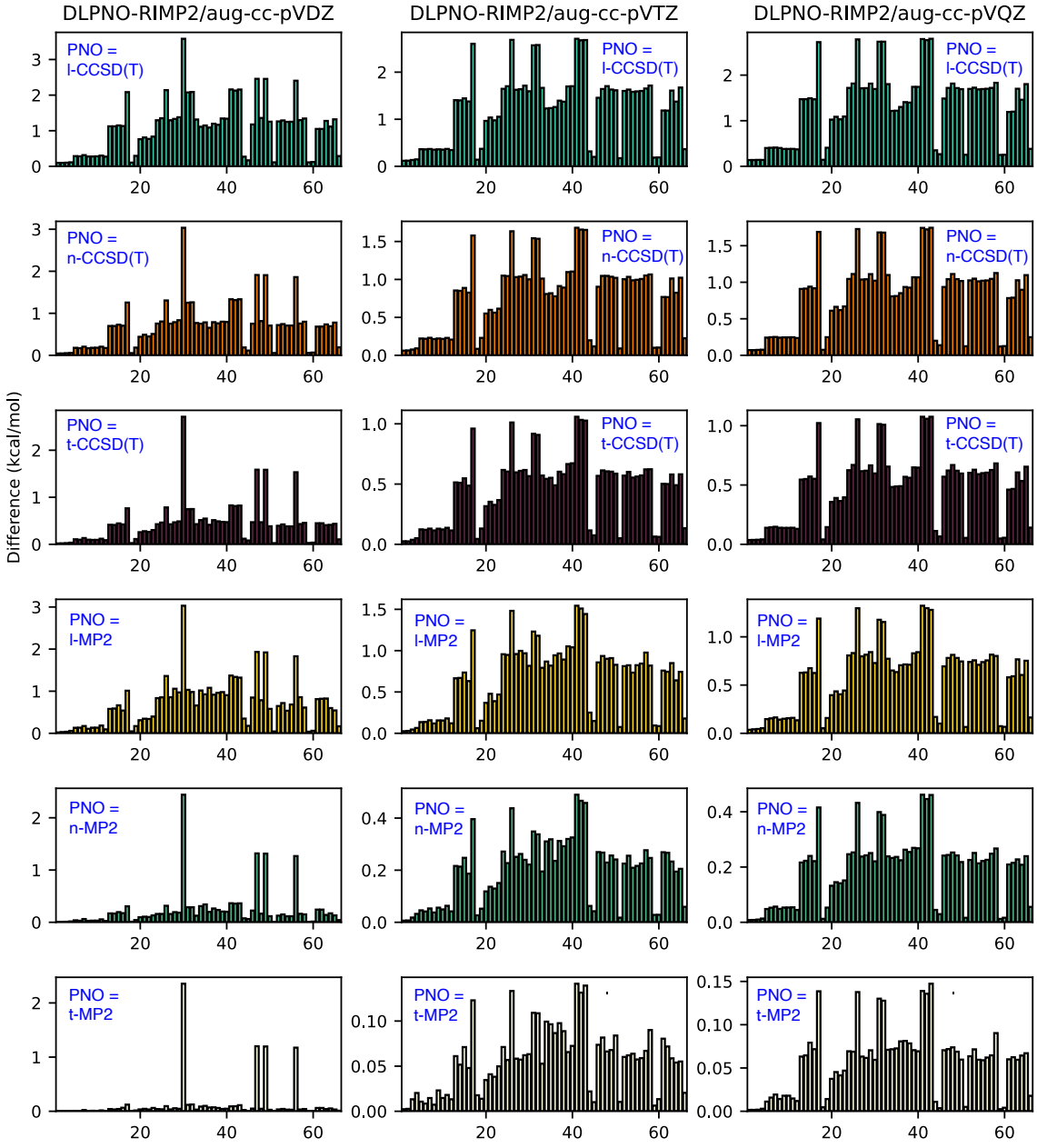

Fig. S17: DLPNO errors in correlation energies monomer #1 of the S66 complexes, computed at the RI-MP2/aug-cc-pVXZ level with PNO thresholds as indicated.

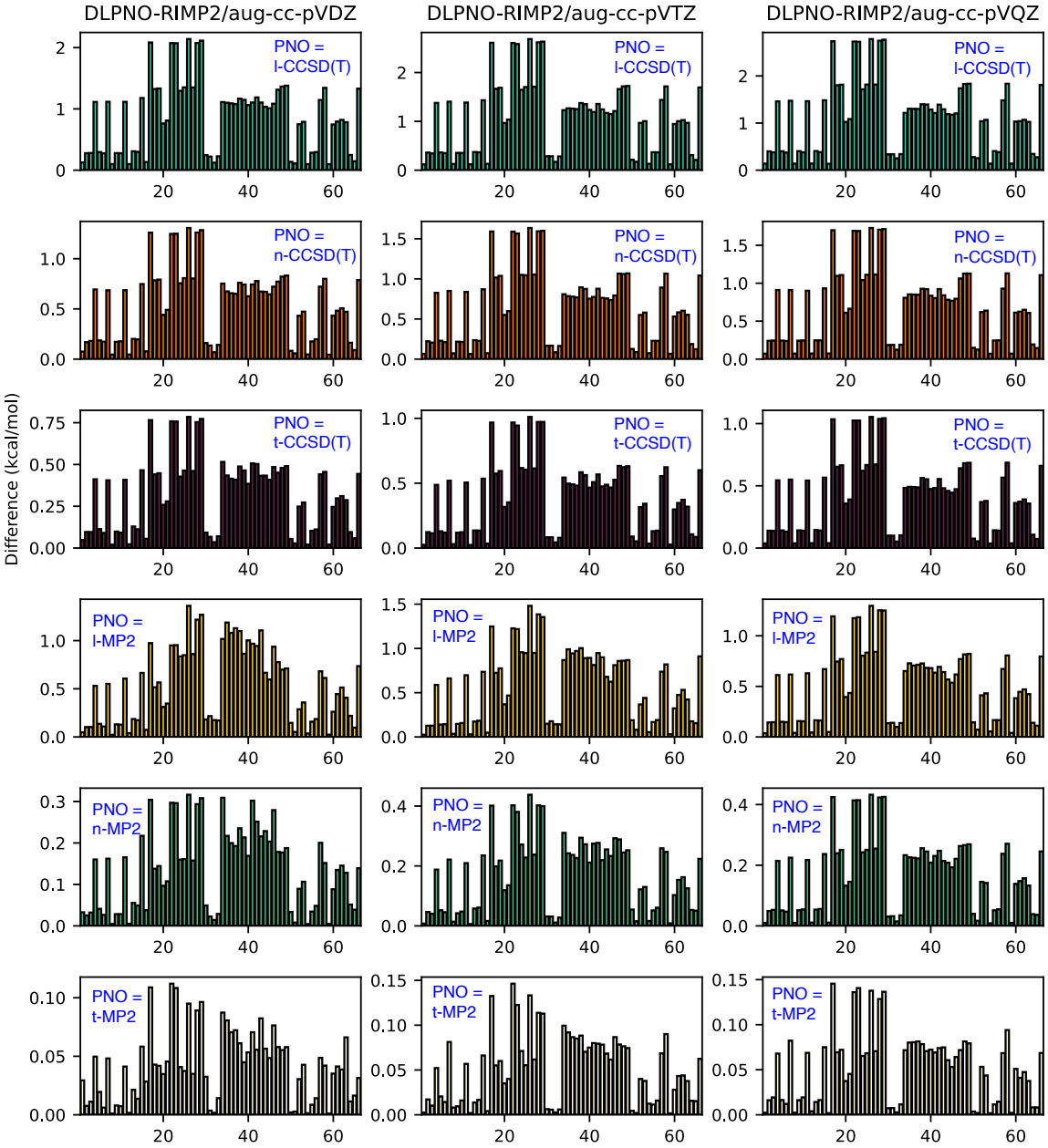

Fig. S18: DLPNO errors in correlation energies monomer #2 of the S66 complexes, computed at the RI-MP2/aug-cc-pVXZ level with PNO thresholds as indicated.

S1.4 MP2/CBS extrapolations

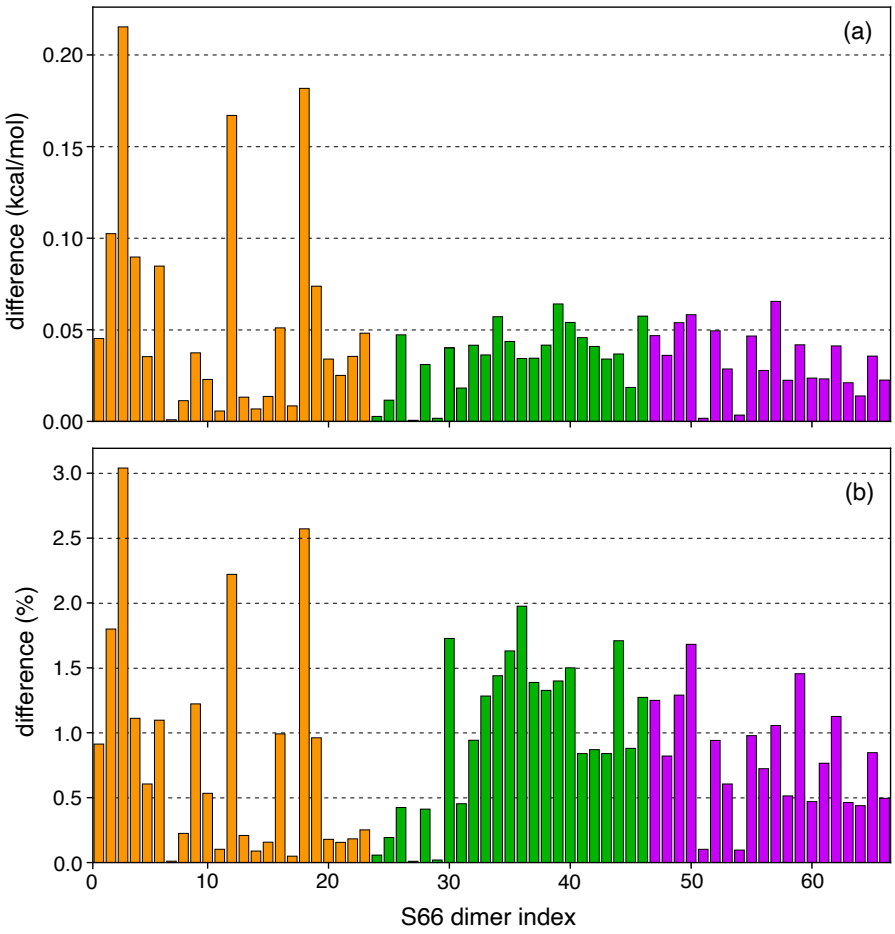

Fig. S19: (a) Absolute and (b) percent differences between CBS-extrapolated RI-MP2 interaction energies for the S66 dimers, comparing cc-pV[T/Q]Z extrapolation to aug-cc-pV[T/Q] extrapolation. Standard subsets of S66 are color-coded as in Figs. 3 and 5.

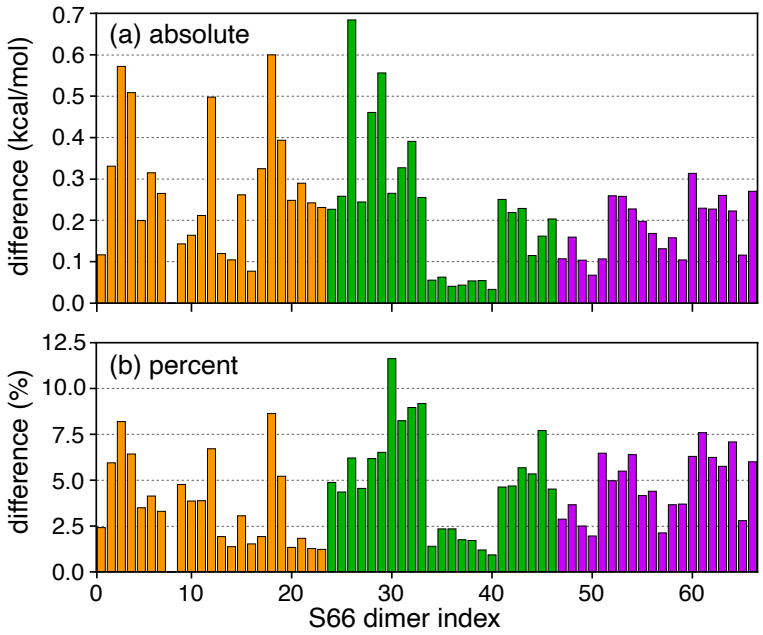

Fig. S20: (a) Absolute and (b) percent differences between RI-MP2/cc-pV[D/T]Z and RI-MP2/aug-cc-pV[D/T]Z interaction energies for the S66 dimers, illustrating the impact of diffuse functions on the CBS extrapolation. Standard subsets of S66 are color-coded as in Figs. 3 and 5.

S1.5 Convergence with PNO threshold

In the following plots, the gray traces show results for each of the individual S66 (L7+BBR) complexes while the dark trace is the average over the entire data set.

S1.5.1 RI-MP2 with Dunning basis sets

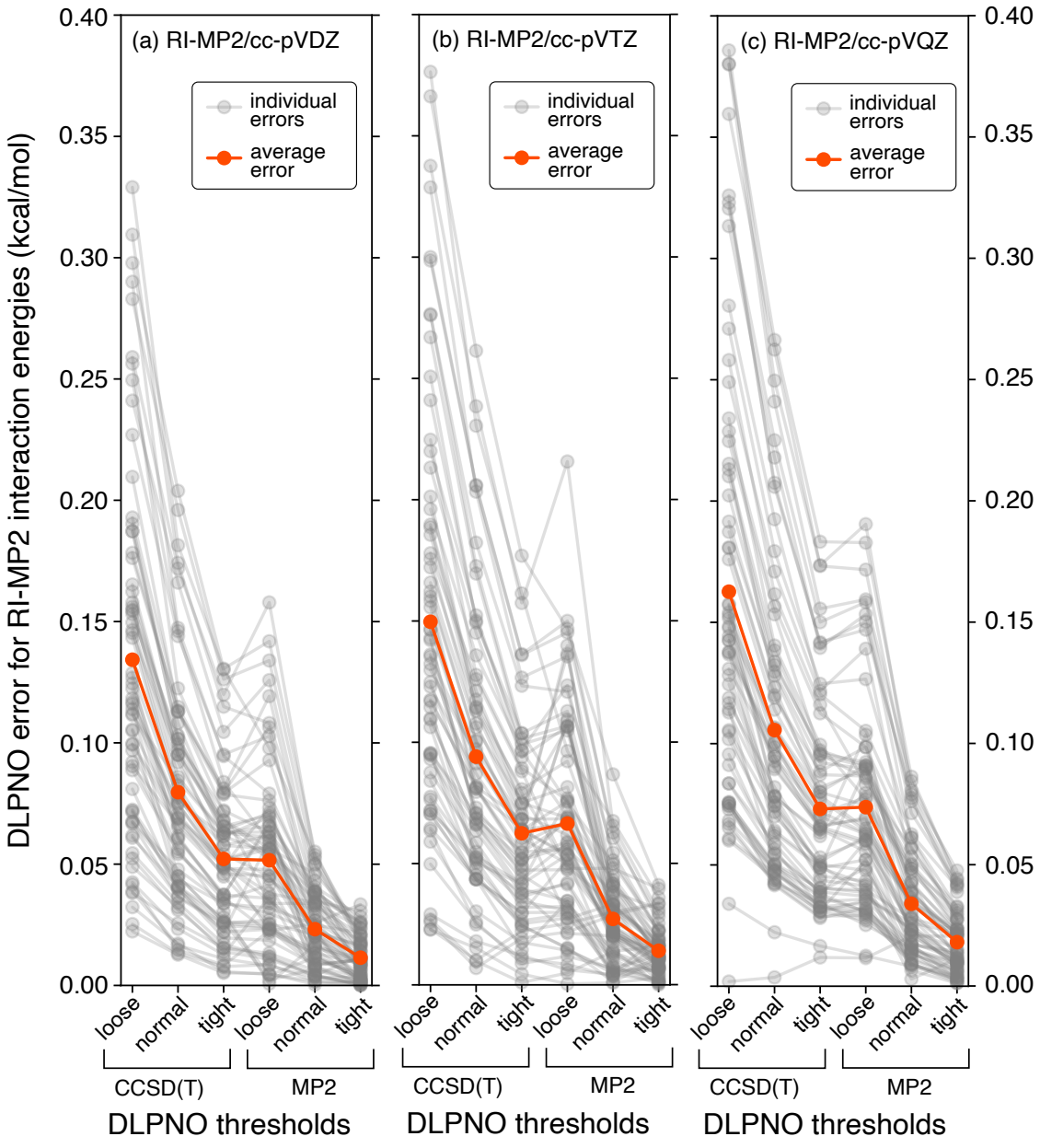

Fig. S21: Absolute DLPNO errors in RI-MP2/cc-pVXZ interaction energies for the S66 complexes.

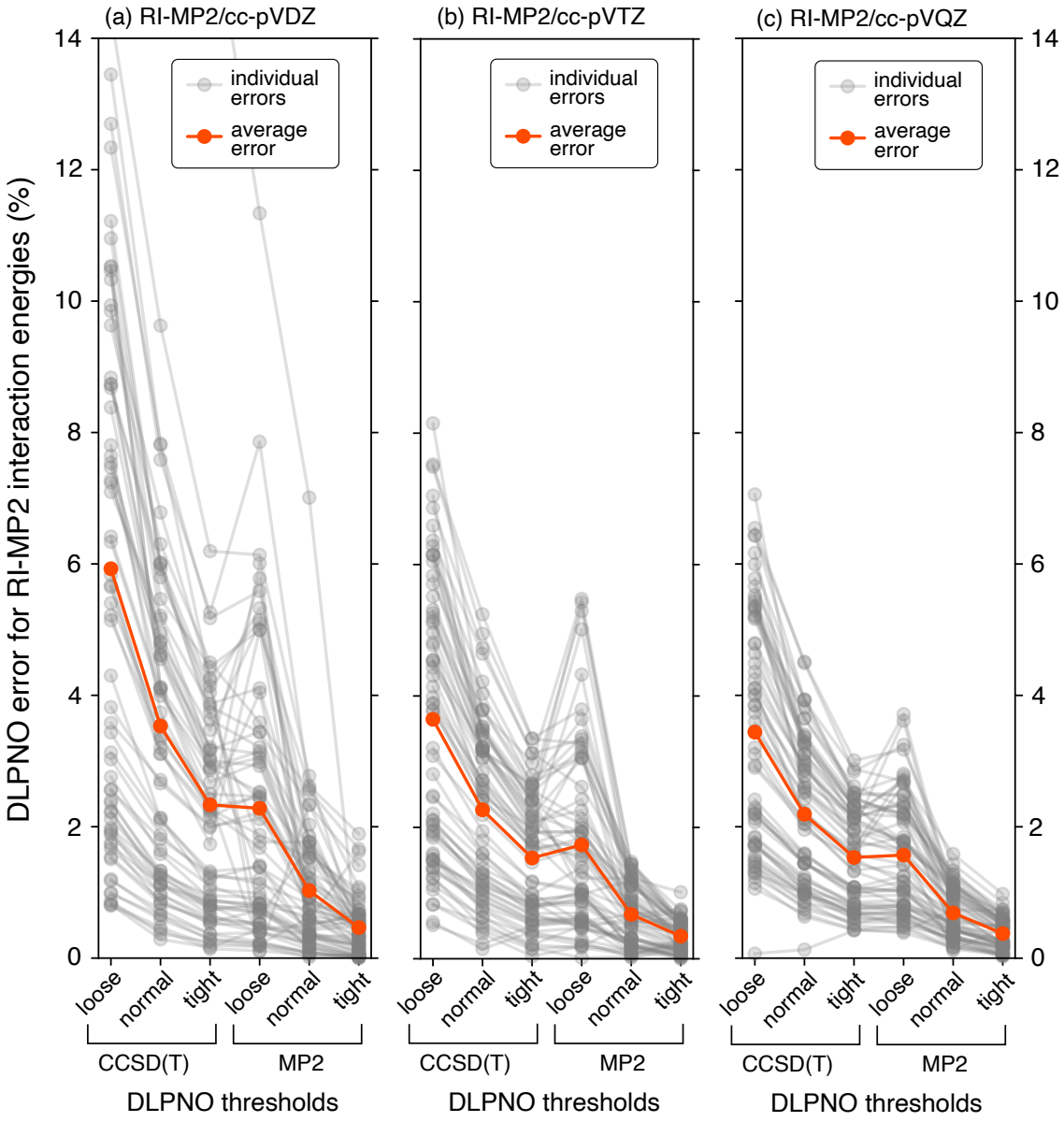

Fig. S22: Percentage DLPNO errors in RI-MP2/cc-pVXZ interaction energies for the S66 complexes.

S1.5.2 RI-MP2 with Karlsruhe basis sets

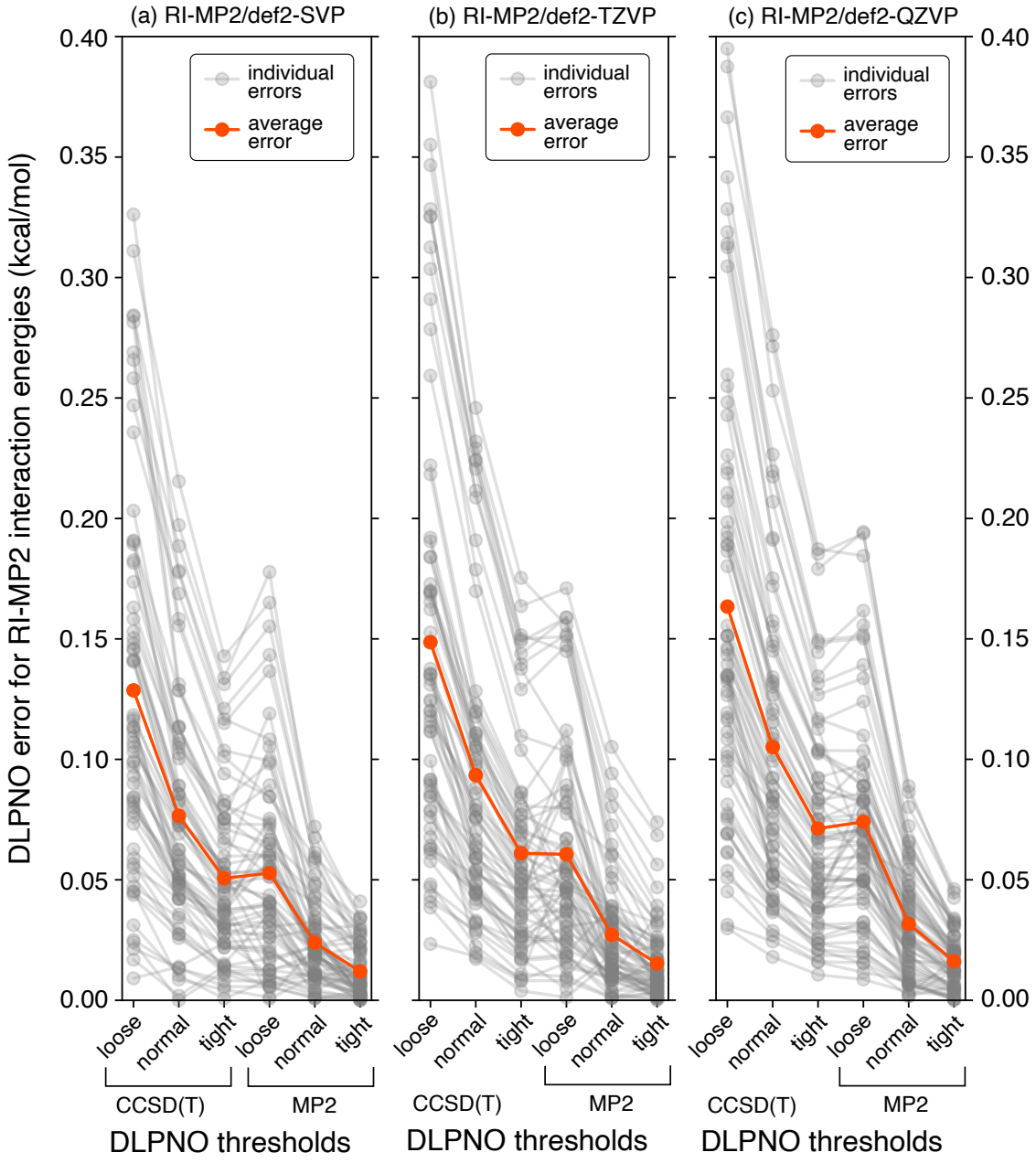

Fig. S23: Absolute DLPNO errors in RI-MP2 interaction energies for the S66 complexes, using Karlsruhe basis sets.

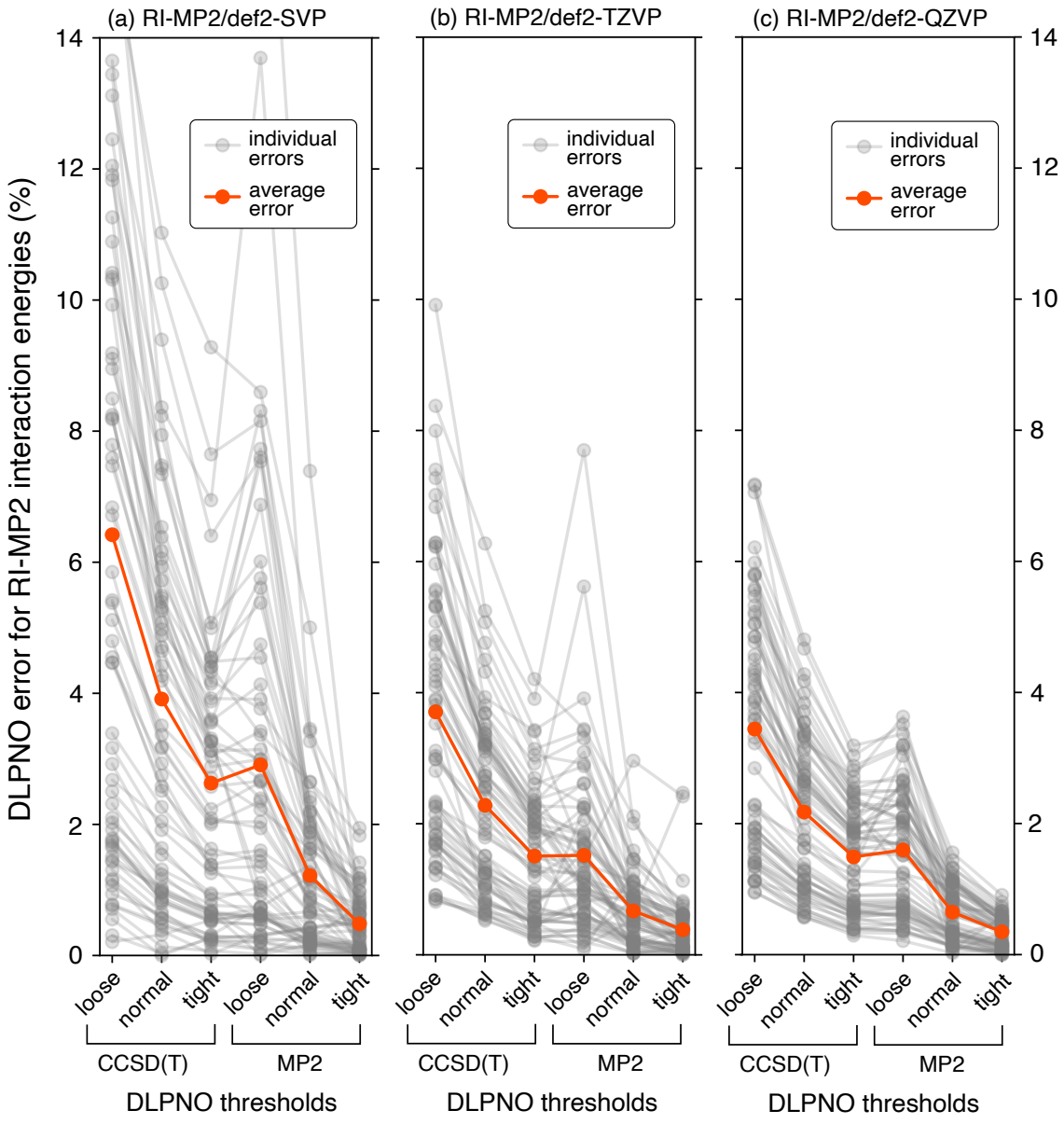

Fig. S24: Percentage DLPNO errors in RI-MP2 interaction energies for the S66 complexes, using Karlsruhe basis sets.

S1.5.3 CCSD(T) data

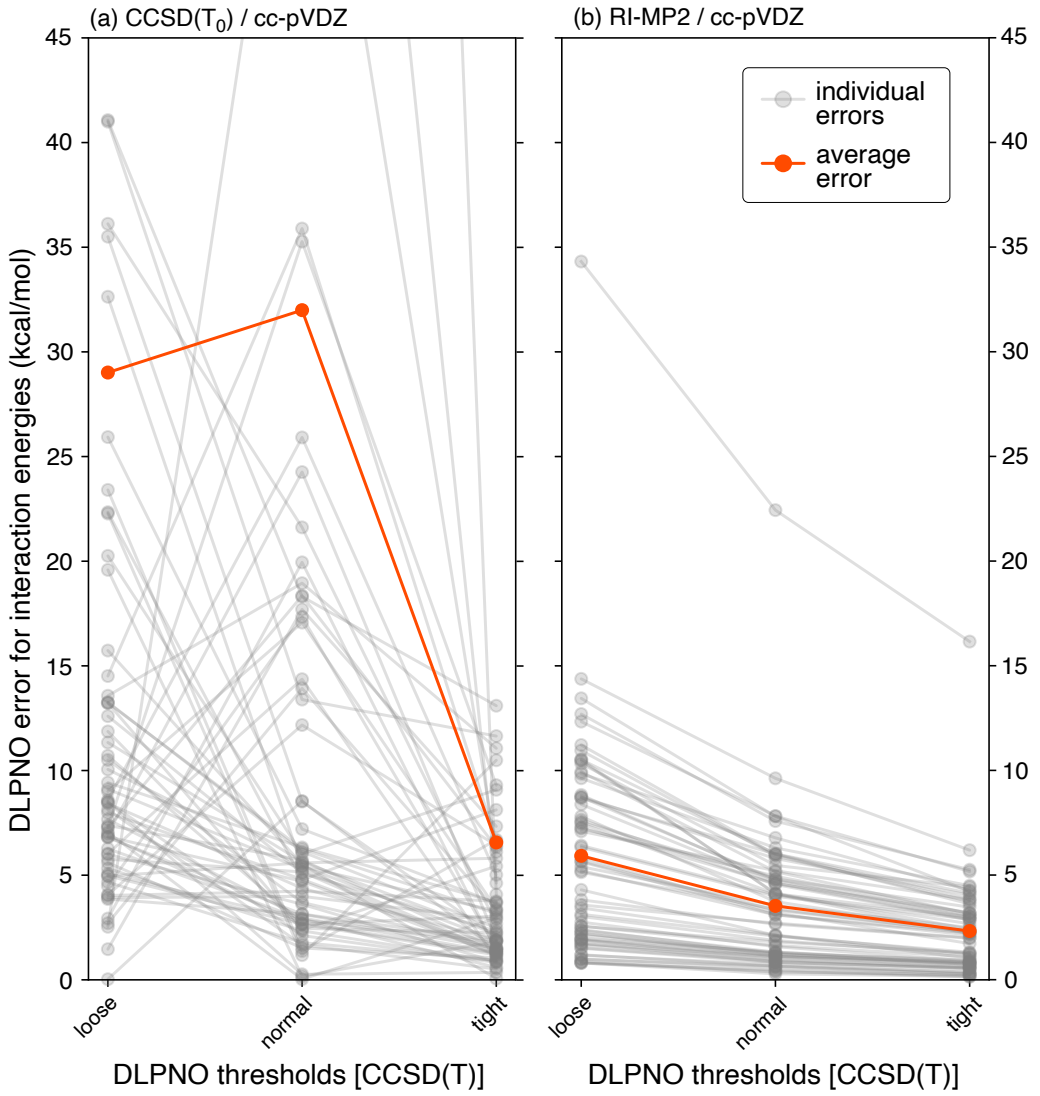

Fig. S25: Percentage DLPNO errors in (a) CCSD(T_0)/cc-pVDZ versus (b) RI-MP2/cc-pVDZ interaction energies for the S66 complexes, using thresholds for CCSD(T).

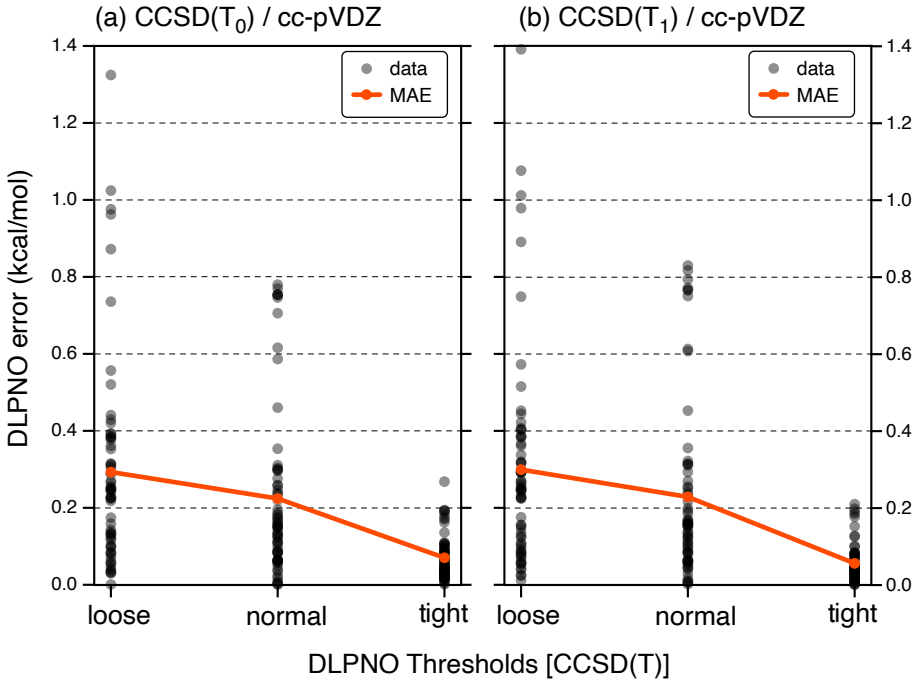

Fig. S26: DLPNO error with respect to the canonical CCSD(T) interaction energies for S66, where the DLPNO-CCSD(T_1) and DLPNO-CCSD(T_0) approximations are used.

S2 Data for Larger Complexes

S2.1 RI-MP2 with Karlsruhe basis sets

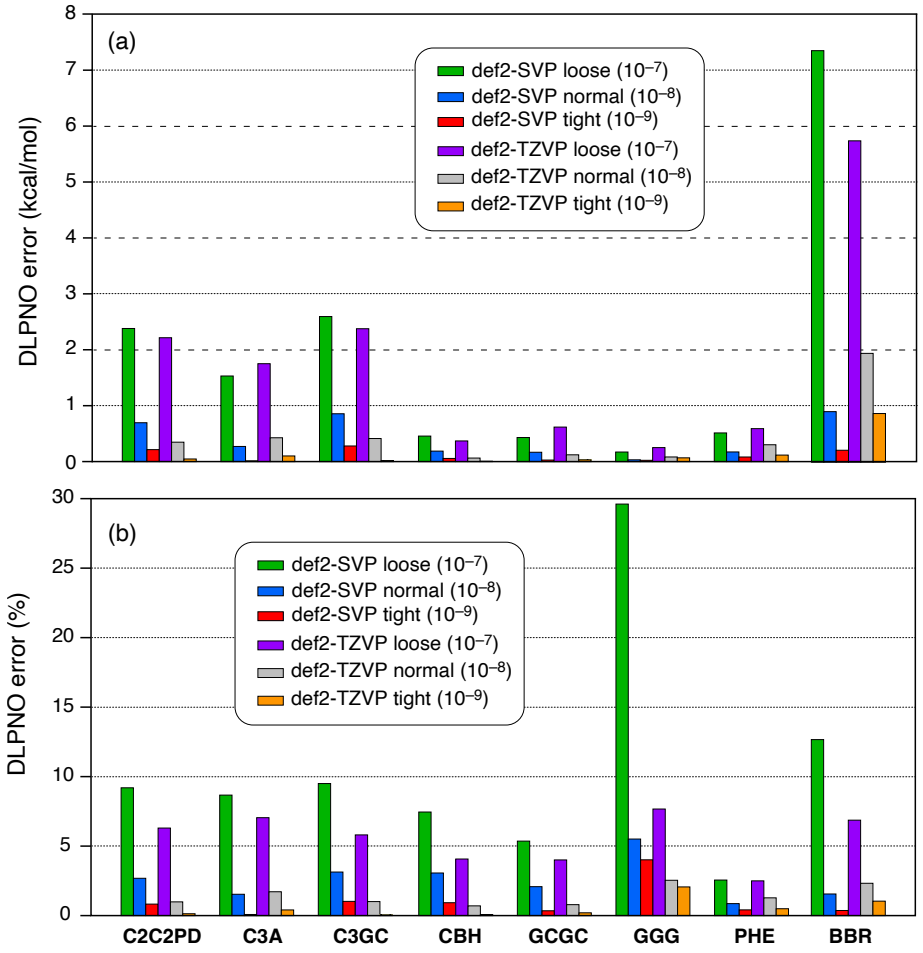

Fig. S27: (a) Absolute and (b) percent DLPNO errors in RI-MP2/Karlsruhe interaction energies for the L7 + **BBR** data set, as a function of the PNO threshold.

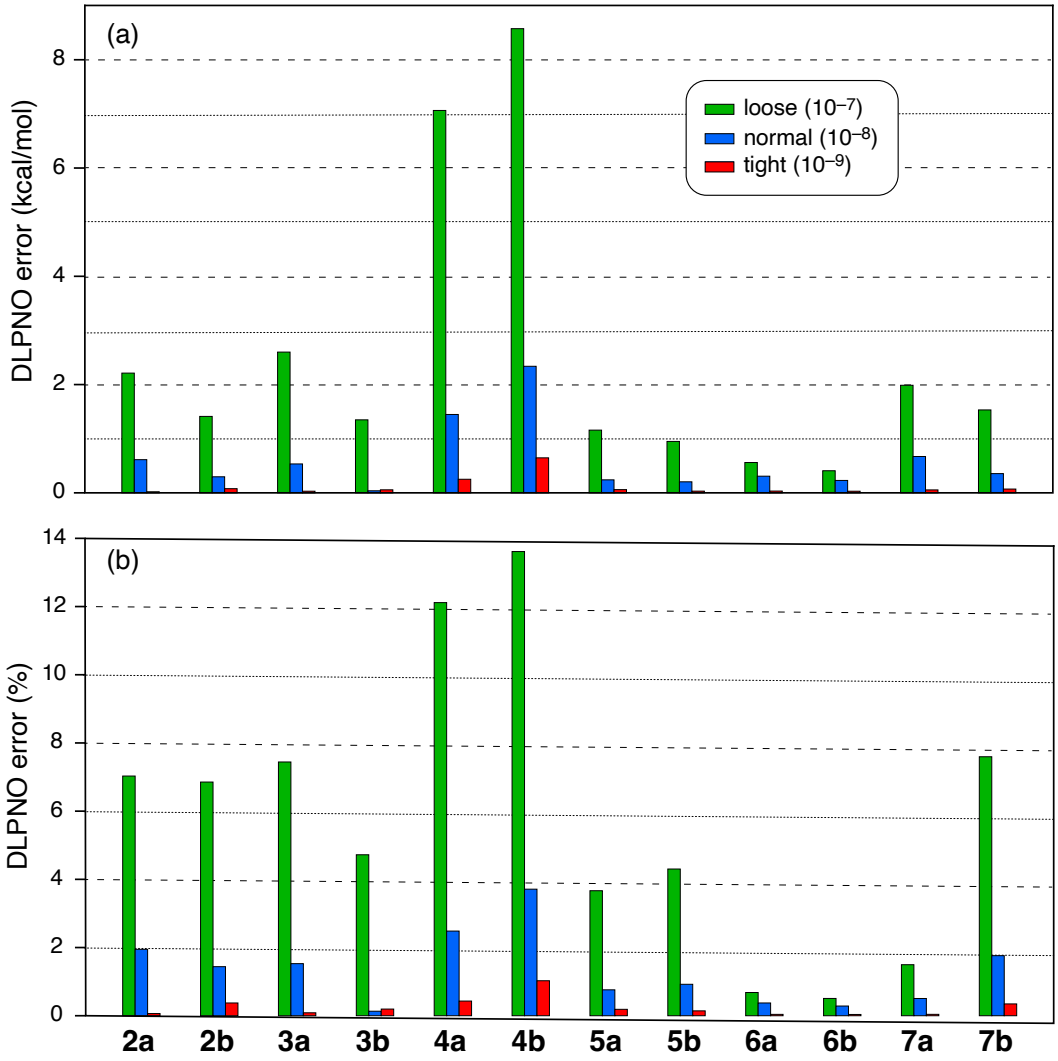

Fig. S28: (a) Absolute and (b) percent DLPNO errors in RI-MP2/def2-SVP interaction energies for the S12L complexes, as a function of the PNO threshold.

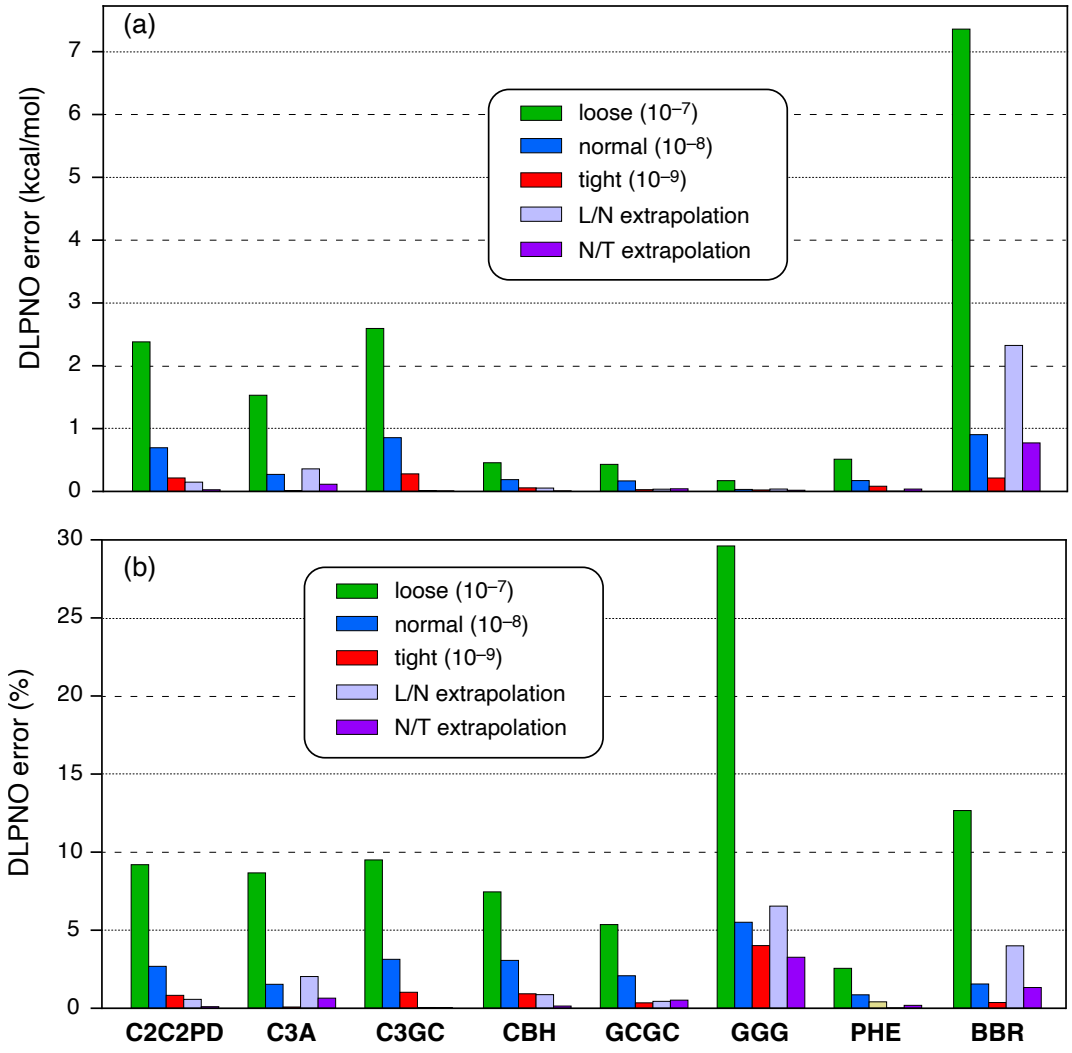

Fig. S29: (a) Absolute and (b) percent DLPNO errors for L7 + **BBR** interaction energies, computed at the RI-MP2/def2-SVP level.

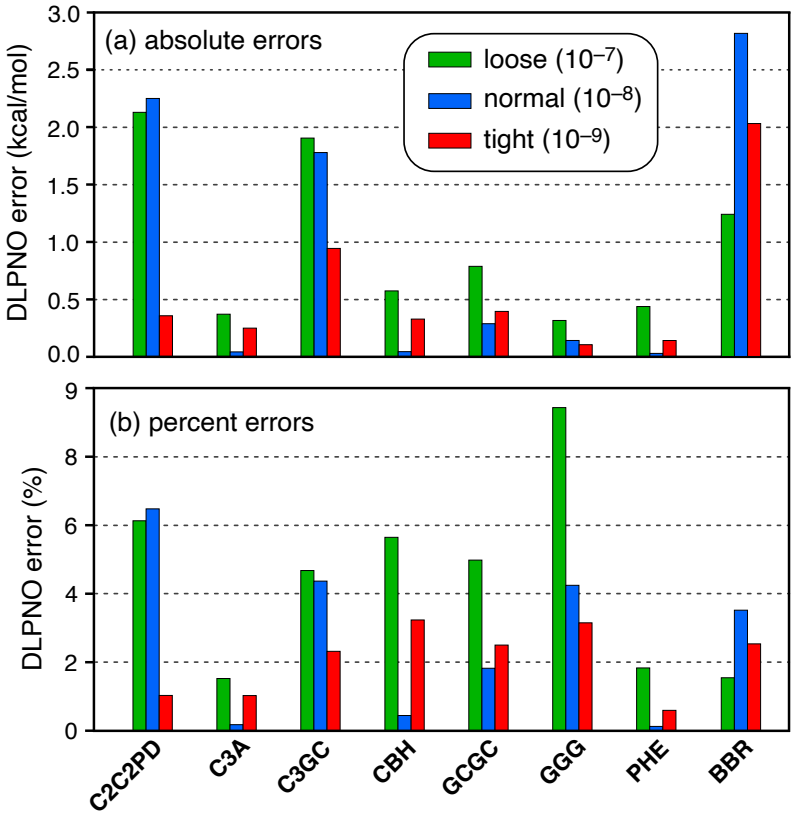

Fig. S30: (a) Absolute and (b) percent DLPNO errors for the L7 + **BBR** data set, computed at the RI-MP2/ def2-SVPD level.

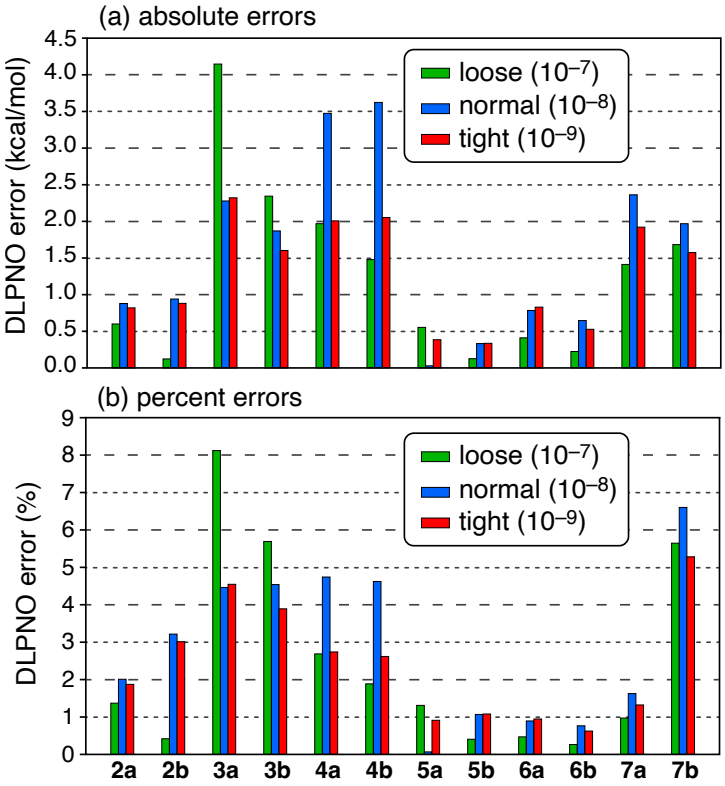

Fig. S31: (a) Absolute and (b) percent DLPNO errors for the S12L complexes, computed at the RI-MP2/ def2-SVPD level.

S2.2 RI-MP2 with Dunning basis sets

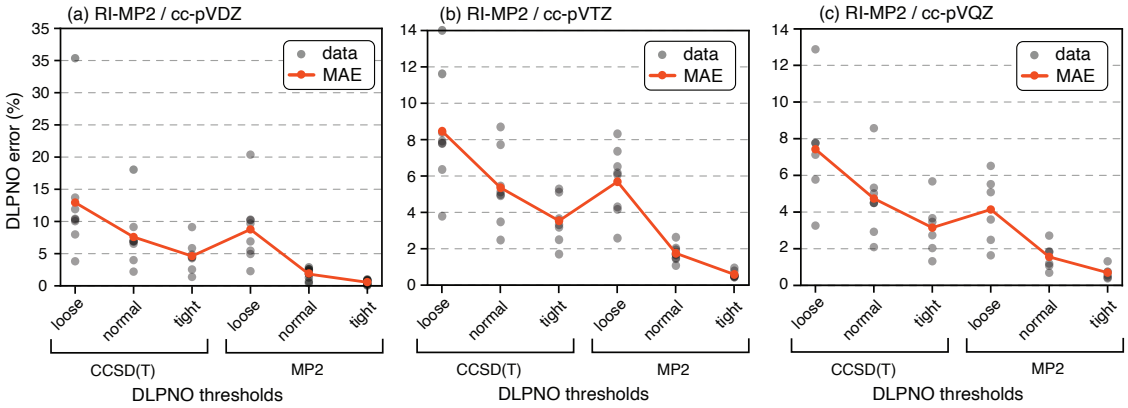

Fig. S32: DLPNO errors, as percentages of ΔE for the L7 + **BBR** complexes, computed at the RI-MP2/cc-pVXZ level.

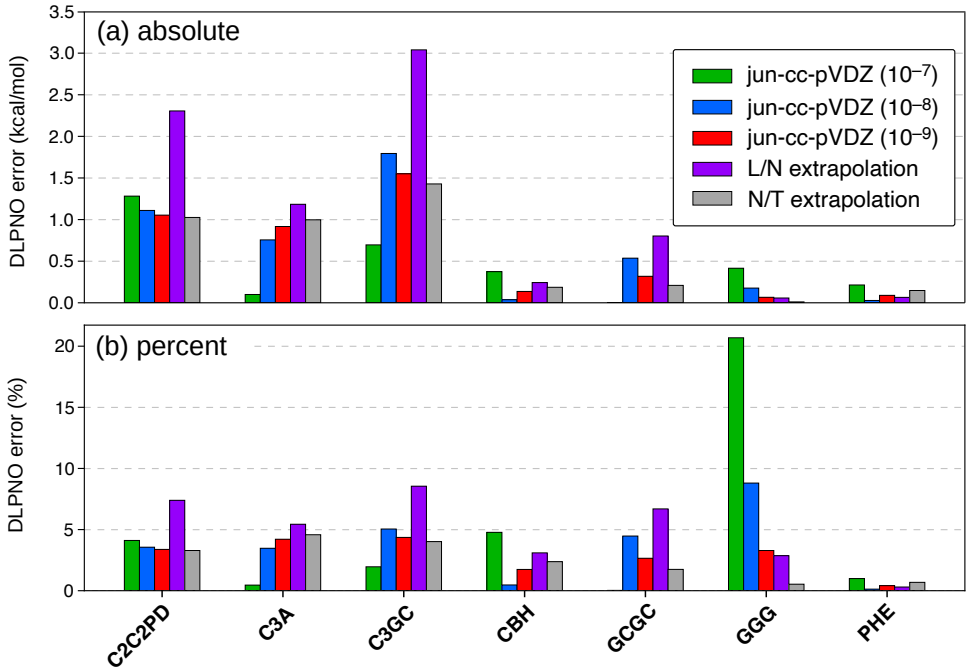

Fig. S33: (a) Absolute and (b) percentage differences between extrapolated DLPNO interaction energies and canonical RI-MP2/jun-cc-pVDZ results, for the L7 complexes.

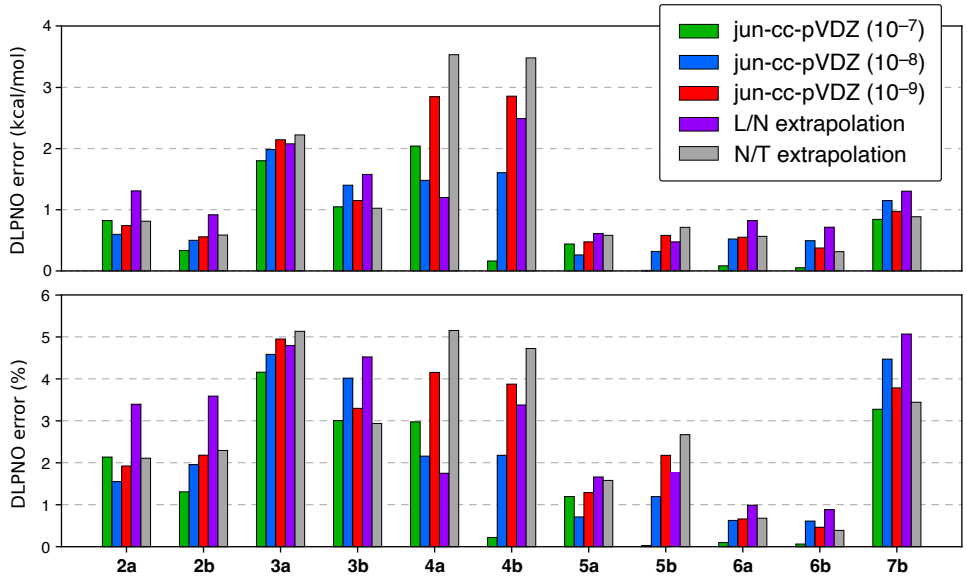

Fig. S34: (a) Absolute and (b) percentage differences between extrapolated DLPNO interaction energies and canonical RI-MP2/jun-cc-pVDZ results, for the S12L complexes.

S2.3 CCSD(T)

Table S1: DLPNO-CCSD(T)/cc-pVDZ interaction energies (in kcal/mol) for the L7 complexes.

Complex	PNO thresholds [CCSD(T) variants]								
	Loose			Normal			Tight		
	T_0	T_1	|diff.|	T_0	T_1	|diff.|	T_0	T_1	|diff.|
C2C2PD	−17.69	−17.54	0.16	−17.62	−17.68	0.05	–	–	–
C3A	−11.30	−11.27	0.03	−12.38	−12.42	0.04	–	–	–
C3GC	−15.31	−15.30	0.00	−19.57	−19.63	0.06	–	–	–
CBH	−4.41	−4.41	0.00	−5.31	−5.31	0.00	−5.74	−5.81	0.07
GCGC	−4.94	−4.89	0.05	−5.98	−5.97	0.02	−4.86	−5.03	0.17
GGG	0.55	0.54	0.01	0.33	0.31	0.02	0.86	0.79	0.07
PHE	−17.09	−17.03	0.06	−17.99	−17.93	0.06	−18.48	−18.51	0.02